Journal of Computer Science Research

Journal of Computer Science Research

Editor-in-Chief

Dr. Lixin Tao

Contents

Articles

ARTICLE

Self-health Monitoring and Reporting System for COVID-19 Patients Using CAN Data Logger

Uttam U. Deshpande[*]   Pooja Hulajatti   Shraddha Suryavanshi   Vrunda Balgi

Department of Electronics and Communication Engg., KLS Gogte Institute of Technology, Belagavi, Karnataka, 590008, India

ARTICLE INFO	ABSTRACT
	In the evolving situation of highly infectious coronavirus, the number of confirmed cases in India has largely increased, which has resulted in a shortage of health care resources. Thus, the Ministry of Health and Family Welfare- Government of India issued guidelines for the 'Home isolation of COVID-19 positive patients' methodology for asymptomatic patients or with mild symptoms. During home isolation, the patients are required to monitor and record the pulse rate, body temperature, and oxygen saturation three times a day. This paper proposes a system that can request data from the required sensor to measure the pulse rate, body temperature, or oxygen saturation. The requested data is sensed by the respective sensor placed near the patients' body and sent to the CAN data logger over the CAN bus. The CAN data logger live streams the sensor values and stores the same to an excel sheet along with details like the patient's name, patient's age, and date. The physicians can then access this information.

1. Introduction

Bosch developed a serial communication protocol called CAN in 1985 to reduce the complex wiring in vehicles. It provides highly efficient and reliable communication between sensors, actuators, controllers, etc. It is a standard network that is preferred in most embedded applications. Previously, CAN was mainly used by the vehicle industry. From then, it is found in almost every automobile ranging from on-road to off-road. Whereas now, the protocol is also widely used in nearly every area of networked embedded controls, with its applications in various products such as medical equipment, building automation, production machinery, weaving machines, wheelchairs, etc. Most medical devices use CAN as an underlying embedded network. This paper presents a Self-health monitoring and reporting system using a CAN logger to monitor the body temperature, oxygen level, and heart rate of COVID-19 patients. CAN data logger is an electronic device used to record the data on the CAN bus over time. A microprocessor with sensors and internal memory forms the base of loggers. These loggers can be stand-alone devices or interfaced with a personal computer through software or user interface.

Presently, the entire world is battling the pandemic of COVID-19. With the increase in the number of affected people, the hospital infrastructure worldwide is insufficient to treat and take care of all the patients. It has led to a situation where asymptomatic patients and patients with

---

Corresponding Author:

Uttam U. Deshpande,

Department of Electronics and Communication Engg., KLS Gogte Institute of Technology, Belagavi, Karnataka, 590008, India;

Email: uttamudeshpande@gmail.com

mild symptoms are isolated at home. However, during this period, the patients must keep track of certain health parameters such as body temperature, oxygen level, and heart rate regularly and report the same. The patient is provided with a thermometer and pulse oximeter separately to record the parameters. This data then needs to be manually updated in the report sheet. Sometimes, this would lead to manipulating the records from the patients' end due to various reasons affecting the patients' health directly.

This paper introduces a system that can read and store physiological parameters and other details about COVID-19 patients. A graphical user interface is provided with the system to create an account for each patient, measure the health parameters, and store the same in an excel sheet. The implementation of the device is categorized into two functional units. The Sensing Unit comprises Arduino UNO, a temperature sensor, and a pulse oximeter. The CAN data logger comprises of STM32F407 microcontroller. The Sensing unit reads sensor data and sends over the CAN bus when requested by the CAN data logger, responsible for displaying it and saving it on the excel sheet through the user interface provided.

2. Literature Review

As illustrated by Priyanka Kakria et al. [1], Veena Sundareswaran et al. [2], and C. Premalatha et al. [3], the Patient monitoring Systems available in the market consists of a microcontroller that could be ATMEGA328 and various health parameter measuring sensors like DS18B20 for temperature, SO00837PS pulse sensor, etc. These systems are plug-and-play devices that collect the data through the sensors and send them to the monitoring system. The monitoring system could be a personal computer, mobile or display interface provided with the device itself. The major setback of using these devices during this pandemic is that the existing devices are not robust. They do not implement any standard secure communication protocol for exchanging the data. These devices are only applicable for personal usage and do not provide any scope to integrate them with the hospital tools and equipment. The devices are mostly capable of only measuring the data and sending it to the monitoring system. Though some systems, as proposed by Prasad Lavgi et al. [4], using CAN protocol, there is no customized application interface that facilitates the patients' data storage.

The systems proposed by K. P. Swain et al. [5], Karumuri Anusha Reddy et al. [6], and Ladlennon C. Banuag et al. [7] uses the CAN protocol to monitor the parameters of multiple patients continuously. In these cases, each patient is required to have the sensing unit always attached to their body. The use of multiple sensing units makes the overall system very expensive.

During this pandemic of COVID-19, it's extremely necessary for the devices being used to be robust, secure, and reliable. Hence, the system illustrated in this paper uses a highly secure CAN protocol for the exchange of data between the sensing node and the data logging unit. This system is interfaced with a customized GUI that provides the medium to log the parameters of multiple patients and is also capable of generating a report that is necessary for analyzing the health of the patient with the timely logged data. The device proposed is designed considering the present coronavirus pandemic situation and is customized in the most suitable form that is useful for the patients in home-isolation and hospitalized.
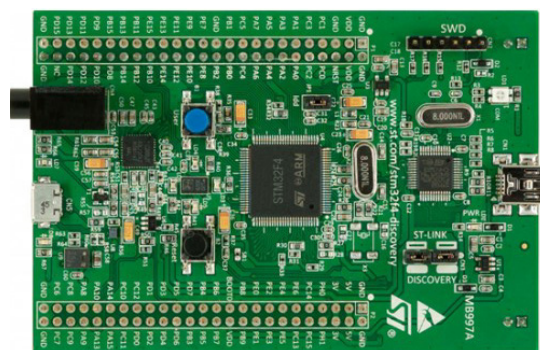
Figure 1. STM32F407VGTx microcontroller

3. Experimental Setup

3.1 Hardware

STM32F407VGTx Microcontroller

Figure 1 illustrates the features of 32F407VGTx Microcontroller. It is a high-performance 32-bit ARM Cortex M4 microcontroller with 100 pins (LQFP100 package). It comes with an FPU core, 1-Mb Flash memory, 192-Kb RAM, and ST-LINK/V2. It also includes LEDs, pushes buttons and a USB OTG micro-AB connector, etc. Various peripherals like ADC, DAC, USART, SPI, I2C, CAN, TIMER, etc., are available [8,9].

MCP2551 CAN transceiver

A high-speed CAN transceiver supports CAN operations of up to 1Mbps with a maximum of 112 nodes connected over the bus and is suitable for 12 V or 24 V operations. It converts the digital signals from the CAN peripheral of a microcontroller to differential signals suitable for the CAN bus and vice versa. It plays a major role in noise-cancellation over the bus [10]. Figure 2 highlights MCP2551 CAN transceiver.

Figure 2. MCP2551 CAN transceiver

FTDI module

It is an USB-to-UART serial converter module and is shown in Figure 3. It has an USB interface, Tx/Rx pins and operates at 3.3 V or 5 V DC. It can be used to convert the data present on USB to serial data suitable for the UART peripheral and vice versa.
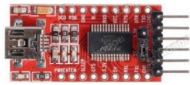
Figure 3. FTDI module

Arduino UNO (ATmega328P)

It is a high-performance 8-bit AVR microcontroller with 32 Kb of Flash memory, 1Kb EEPROM, 2 Kb internal SRAM. It operates at a voltage of 2.7 V-5.5 V and a temperature range of $-40°C$ to $+125°C$. It has many integrated peripherals like TIMERS, PWM, ADC, UART, SPI, etc. A variety of sensors and actuators can be integrated to sense and control the external environment. The Figure 4 indicates the Arduino UNO (ATmega328P) microcontroller.

Figure 4. Arduino UNO

MCP2515 CAN shield

It is a CAN controller module with an SPI interface.

It implements the CAN protocol v2.0B with a baud rate of up to 1Mbps. It can transmit and receive both standard and extended CAN frames. It can be used to provide external CAN support on a microcontroller by interfacing it through SPI [11]. Figure 5 displays MCP2515 CAN shield.

Figure 5. MCP2515 CAN shield.

LM35 Temperature sensor

It is a precision temperature device with 3-terminals as shown in Figure 6. It produces an analog voltage that is linearly proportional to the temperature in centigrade. It can accurately measure temperature in the range of $-55°C$ to $+150°C$.

Figure 6. LM35 Temperature sensor

MAX30102 Pulse oximetry and Heart-rate monitor module

It is used to monitor heart rate and oxygen saturation level in the blood. It is integrated with two LEDs, a photodetector, low noise analog signal processing and optimized optics. It operates within the voltage range of 1.7 V-2 V. It outputs the heart-rate in BPM and the oxygen saturation level in percentage [12]. Figure 7 highlights MAX30102 module.

Figure 7. MAX30102 module.

3.2 Software

Keil µVision 5

It is free software used for embedded software development. It is an Integrated Development Environment (IDE) with a text editor, compiler, and hex code generator. It allows verification of the code using the simulator, load the code into the microcontroller and validate the working using the debugger. The peripheral registers can also be

viewed on the debugger.

Arduino 1.8.9

It is a cross-platform used by developers to write and upload codes in Arduino boards. It provides an interface to include libraries and program different sensors, compile and upload code to Arduino-compatible boards, views the results using Serial monitor and Serial plotter options.

Microsoft Visual Studio 2019

It is an IDE used to develop GUIs, websites, apps, web services, and computer programs using software development platforms like Windows forms, Windows API, Microsoft Silverlight, etc. It includes a code editor, code refactoring, code profiler, debugger, GUI designers, web, class, etc.

3.3 Communication Protocol

CAN Protocol

It is a message-based, broadcast-type protocol with differential two-wired communication (CAN_H and CAN_L). It is a multi-master, asynchronous, serial communication facility defined by International Standards Organization (ISO). CAN bus supports data speeds up to 1 Mbps. The CAN_H and CAN_L lines are terminated by 120Ω resistance on either side to reduce the signal reflection. Due to its high performance and the ease of adding or deleting the nodes, the CAN bus is considered a flexible system. Each node can send and receive messages on the bus but not simultaneously. These messages follow the Standard CAN frame format defined under ISO-11898 [13].

UART

Universal Asynchronous Receiver Transmitter is a circuit used for serial communication. It transmits the data asynchronously by using only two wires. The transmitting UART converts the parallel data into serial, and receiving UART converts serial data back into parallel. The transmitting UART attaches additional Start and Stop bits to the 8-bit data package, indicating the start and end of data for receiving UART.

3.4 Block Diagram

The proposed system shown in Figure 8 mainly consists of two units, the Sensing unit where all the sensors i.e., the LM35 Temperature sensor read the body temperature. The MAX30102 Pulse oximetry and Heart-rate monitor module read heart rate and oxygen saturation level. They are connected with the CAN data logger and

GUI used to log and store the physiological parameters of multiple patients.
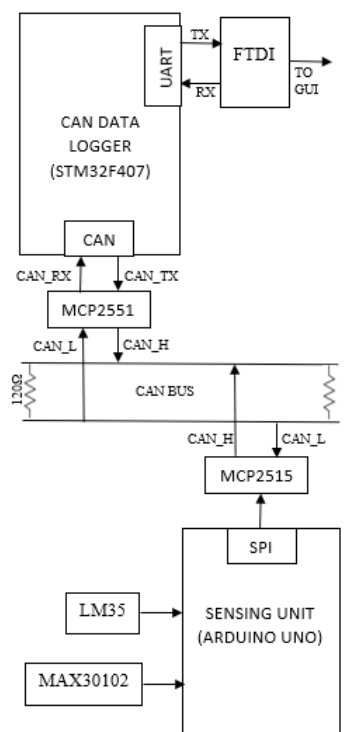
Figure 8. Block diagram

The CAN data logger communicates to the Sensing unit over the CAN bus, and the GUI communicates with the CAN data logger through UART.
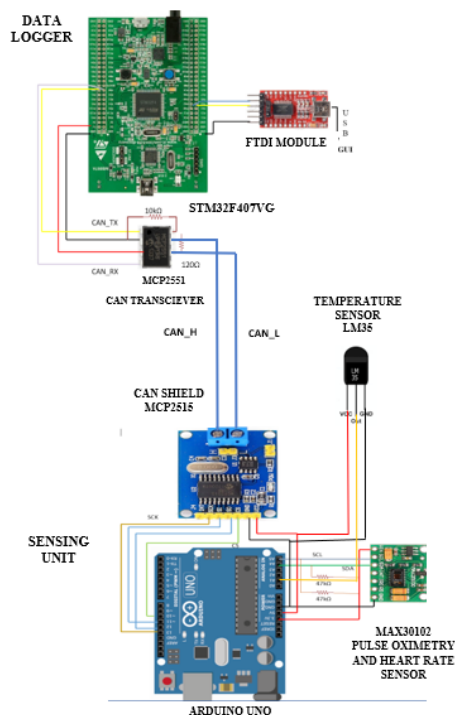
Figure 9. The layout of the proposed system.

4. Implementation

Sensing unit

The microcontroller used is Arduino UNO (ATmega328P). The LM35 temperature sensor, the MAX30102 module is interfaced with it to read the body temperature and heart-rate + oxygen saturation level, respectively. The MCP2515 CAN shield interfaced to communicate over the CAN bus. The sensing unit responds to the CAN data logger's request by reading the data from sensors and sending it over the CAN bus. Figure 9 illustrates the layout of the proposed system.

CAN data logger

The microcontroller used is STM32F407VGTx. It is the main unit that logs and stores the sensor data. The FTDI module and the MCP2551 CAN transceiver are interfaced with GUI through UART and over CAN bus.

When the user selects a particular sensor on GUI, it sends a CAN remote frame requesting sensor data to the Sensing unit. It then reads the response CAN message and displays the sensor data on GUI.

GUI

The GUI provides means to interact with the CAN data logger. The patient can create an account, log in to log sensor data, and view previous records. It also provides an inference of the logged data. Multiple patient records can be stored, which can be accessed only by the doctor. The GUI stores details of the patient like name, patient ID, age, gender, address, etc. Figure 10 and 11 displays the flow diagram sensing unit and data logging units.

5. Results

The hardware setup for the proposed system is shown in Figure 12.
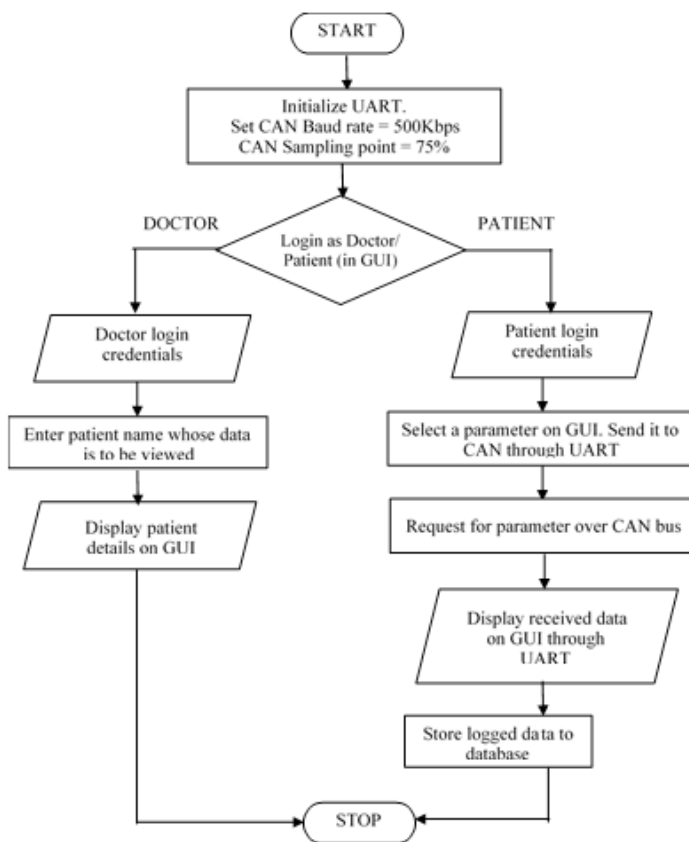
Figure 10. Process flow of Sensing unit.
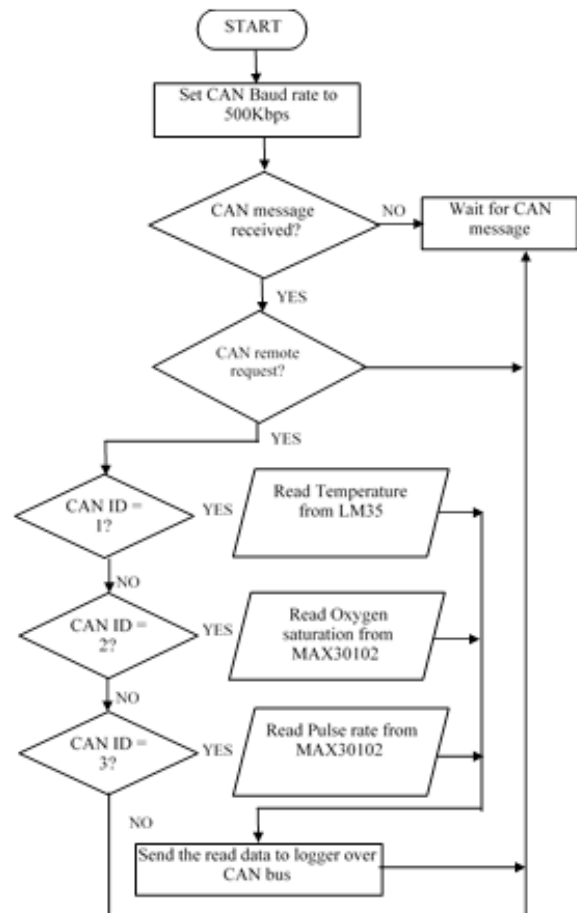
Figure 11. Process flow of CAN data logger and GUI.
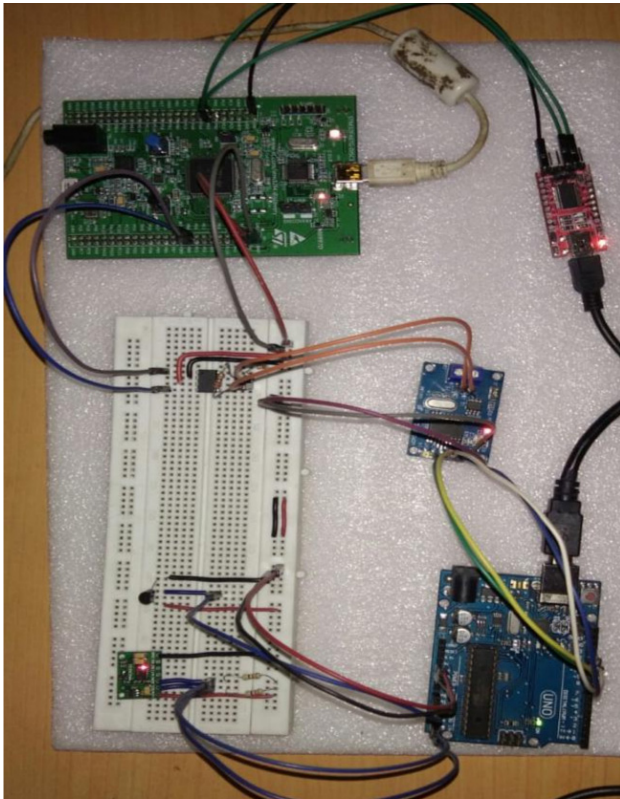
Figure 12. The hardware setup of the proposed system

A registration page is provided for every new patient to enter his/her details. It creates an excel sheet to store data of that particular patient.

Figure 13. Registration page for new user

After creating an account, the patient has to login with a name and ID to log the health parameters.

Figure 14. Login page for patient

When a user is successfully logged-in, the patient has to place the index finger on the sensor. The GUI provides the option to measure and save the body temperature, blood oxygen level, and heart rate. It also gives an overall inference of patients' health. The patient can also view his previous records.

Figure 15. Option to log, save and view records

The doctor can view details of any patient by logging-in though with his credentials and enter the patient name and ID. Figures 13 to 17 show the snapshots of the patient registration and data logging procedures.

Figure 16. Interface for doctor

Figure 17. Logged data saved to excel sheet

6. Conclusions

The paper successfully shows the implementation of the patient health parameter monitoring system, which is capable of measuring the body temperature, heart rate, and oxygen level of the patient. The device has been interfaced with a GUI capable of requesting the sensor data and adding the requested data to the excel sheet to generate the report with timely logged data. The system illustrated is designed to keep the present coronavirus pandemic situation in mind with an intention to provide a robust, secure, and low-cost solution for keeping track of both the patients in hospital and patients under home isolation.

References

[1] Priyanka Kakria, N. K. Tripathi, and Peerapong Kitipawang, "A Real-Time Health Monitoring System for Remote Cardiac Patients Using Smartphone and Wearable Sensors", International Journal of Telemedicine and Applications Volume 2015, Article ID 373474, 2015.

[2] M. Saranya, R. Preethi, M. Rupasri and Dr. S. Veena. "A Survey on Health Monitoring System by using IOT", International Journal for Research in Applied Science & Engineering Technology, Volume-6, Issue-III, , pp. 778-782, 2018.

[3] C. Premalatha, R.P. Keerthana and R. Abarna. "Human Health Monitoring System", International Research Journal of Engineering and Technology, Volume-6, Issue-1, pp. 914-916, 2019.

[4] Prasad Lavgi and Mr. Lakshaman Kora, "Patient Health Monitoring System using CAN Protocol", International Research Journal of Engineering and Technology, Volume-6, Issue-6, pp. 394-398, 2019.

[5] K.P. Swain, M.V.S. V Prasad, J. Sahoo, S. K. Sahoo, G. Palai, "Patient Monitoring System using CAN and Android", Journal of Research in Science, Technology, Engineering and Management, pp. 101-105, 2016.

[6] Karumuri Anusha Reddy and Narendra Babu Tatini, "Monitoring of Patients Health in Hospitals using CAN Protocol", International Journal of Innovative Technology and Exploring Engineering, Volume-8, Issue-6, April 2019, pp. 1556-1559.

[7] Ladlennon C. Banuag and Joseph Karl G. Salva, "Development of a Patient Monitoring System for Hospital Wards Employing Zigbee Technology and CAN Protocol", 2019 2nd World Symposium on Communication Engineering (WSCE), Nagoya, Japan, pp. 112-116, 2020.

[8] STMicroelectronics, "STM32F405xx and STM-32F407xx, ARM Cortex-M4 32b MCU+FPU, 210DMIPS, up to 1MB Flash/192+4KB RAM, USB OTG HS/FS, Ethernet, 17 TIMs, 3 ADCs, 15 comm. interfaces & camera", DocID022152 Rev 8 datasheet, 2016.

[9] STMicroelectronics, "STM32F405/415, STM32F407/417, STM32F427/437 and STM32F429/439 advanced Arm®-based 32-bit MCUs", RM0090 Rev 17 reference manual, 2018.

[10] Microchip Technology Inc., "MCP2551, High-Speed CAN Transceiver", DS21667F datasheet, 2010.

[11] Microchip Technology Inc., "MCP2515, Stand-Alone CAN Controller With SPI™ Interface", DS21801D datasheet, 2005.

[12] Maxim Integrated Products, Inc., "MAX30102, High-Sensitivity Pulse Oximeter and Heart-Rate Sensor for Wearable Health", 2015.

[13] Steve Corrigan, "Introduction to the Controller Area Network (CAN)," Texas Instruments, SLOA101B application report, 2016.

ARTICLE

Unmanned Drug Delivery Vehicle for COVID-19 Wards in Hospitals

Uttam U. Deshpande[1*] **Aditya Barale**[1] **V. S. Malemath**[2]

1. Department of Electronics and Communication Engg., KLS Gogte Institute of Technology, Belagavi, Karnataka, India
2. Department of Computer Science and Engineering, KLE Dr. M.S. Sheshgiri College of Engineering and Technology, Belagavi, Karnataka, India

ABSTRACT

The prime reason for proposing the work is designing and developing a low-cost guided wireless Unmanned Ground Vehicle (UGV) for use in hospitals for assistance in contactless drug delivery in COVID-19 wards. The Robot is designed as per the requirements and technical specifications required for the healthcare facility. After a detailed survey and tests of various mechanisms for steering and structure of UGV, the best mechanism preferred for steering articulated and for body structure is hexagonal as this approach provides decent performance and stability required to achieve the objective. The UGV has multiple sensors onboard, such as a Camera, GPS module, Hydrogen, and Carbon Gas sensor, Raindrop sensor, and an ultrasonic range finder on UGV for the end-user to understand the circumferential environment and status of UGV. The data and control options are displayed on any phone or computer present in the Wi-Fi zones only if the user login is validated. ESP-32 microcontroller is the prime component utilized to establish reliable wireless communication between the user and UGV.

These days, the demand for robot vehicles in hospitals has increased rapidly due to pandemic outbreaks as using this makes a contactless delivery of the medicinal drug. These systems are designed specifically to assist humans in the current situation where life can be at risk for healthcare facilities. In addition, the robot vehicle is suitable for many other applications like supervision, sanitization, carrying medicines and medical equipment for delivery, delivery of food and used dishes, laundry, garbage, laboratory samples, and additional supply.

1. Introduction

A guided Unmanned Ground Vehicle (UGV) is a type of Robotic assistance vehicle. The accurate guidance from system or human makes the operating vehicle easy over a wide variety of terrains and capacity to perform a wide variety of tasks in place of humans but with human or system supervision. Unmanned robotics are effectively created for regular citizens and military use to serve dull, grimy, and hazardous tasks. Unmanned Ground Vehicle' is classified into two types:

1) Tele-operated: A Tele-operated UGV is a vehicle that a human administrator constraint at a distant area

---

employing communication links. The administrator gives every psychological procedure, dependent on sensor feedback from either viewing visual perception or input from the sensor, such as camcorders [7].

2) Self-governing: A self-governing UGV is an autonomous robot that is entirely self-ruling and self-correcting in most cases.

The Robotic vehicle (UGV) that we made tests the feasibility and efficacy of surveillance and environmental study. The robot assists guidance program made by us relays the ecological parameters and stores a set of data for suggestions in a similar scenario in the future. The data include the convergence of gases in the environment, like hydrogen and Carbon monoxide. Detection of humidity and temperature is also recorded. This gives humidity and temperature to the surrounding air. Nowadays, the interest in robots and their utilization in clinics have expanded because of segment patterns and clinical cost control changes. The most important current contagious pandemic can risk one's life. These robotized frameworks are structured explicitly to deal with mass material, drug medications, and transportation of food, grimy dishes, bedding, garbage, and biomedical instruments for medical management provisions. A processor is used with a few sensors, including a RF transmitter for communication over Wi-Fi using ESP-32 to study and act in the environment.

2. Literature Review

The following passages show the survey done by our group on the vast literature relating to the UGV's. The literature includes work carried out by various researchers. The survey may also include information from different authentic internet websites. To keep the literature survey simple, we have briefly summarised the work carried out by researchers. The following passages show the survey done by our group on the vast literature relating to the UGV's. The literature includes work carried out by various researchers. The survey may also include information from different authentic internet websites. To keep the literature survey simple, we have briefly summarised the work carried out by researchers.

A generalized kinematic modeling approach for mobile robots with the articulated steering mechanism was exhibited by F. Le Menn et. al., [1]. The proposed formulation for inferring the I/O equations of such kinematic structures extends the reciprocating screw method of asymmetric and constrained parallel mechanisms. The efficiency of this methodology in establishing the differential kinematics model is demonstrated by an application: the "RobuRoc" mobile robot. Its intricate kinematic structure is initially transformed into a parallel spatial mechanism encapsulating the differential drive wheel system. The analytical shape of the reciprocating screw system corresponding to the active control wrenches applied to the controlled body is established. The reciprocal screw system is the analytical form that fits in the actively managed wrenches used to establish regulated functions in the body. Conversely, it outlines how wheel speeds are transferred to the output body. It also provides geometric information for an exhaustive analysis of the singularity and optimizes traction distribution when highly irregular surfaces evolve. From the differential drive kinematic model, the traction ellipsoid concept is utilized for evaluating the impediment clearance capabilities quantitatively when the pattern of the total system and the contact circumstances are notably variable.

Valjaots et. al., [2] examined the energy efficiency of Unmanned Ground Vehicles (UGVs). The vehicle platform's energy efficiency depends entirely on the designed elements and the surrounding environment where it is to be used. The efficiency also depends on the navigation algorithms used. For confirmation of all UGV design factors that have a measurable effect on energy efficiency comprises an integrated measuring system to obtain the vehicle's dynamic motion and interaction with environmental factors during the real-time test mission. Various design profiles are used to improvise and optimize the efficiency of UGV and a control system. The results obtained are applied to the development, simulation, and testing library used as a product design medium in an early phase.
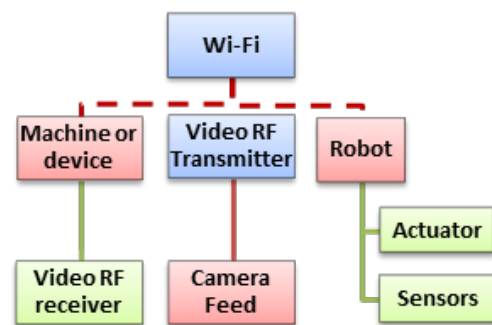
Figure 1. Block Diagram.

3. System and Control Architecture

The above block diagram in Figure 1 illustrates system architecture. A wireless router, also called a Wi-Fi router, combines a wireless access point and a router's networking functions. The router helps guide the robot for free movement in the hospital wards. Here, the Wi-Fi router acts as a bridge between the client and the robot. The next part explains the onboard components used in building the robot.

3.1 On-Board Components
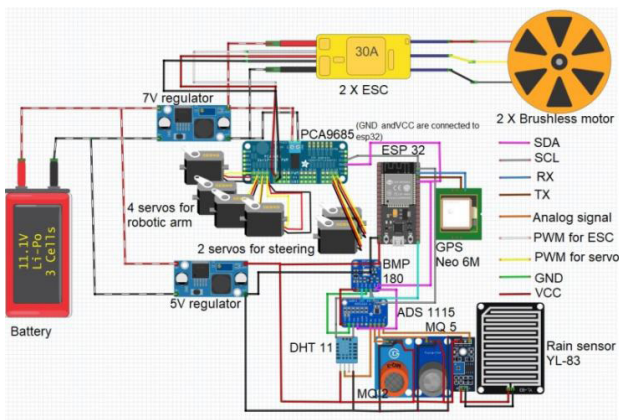
Figure 2. On Board components.

Figure 2 describes the components used in building our Robot, and Figure 3 illustrates the devices used to create the base station. The onboard device used are ESP 32, BMP 180 Pressure Sensor, NEO-6MV2 GPS Sensor, Gas Sensor MQ2 and MQ7, DHT11 temperature and humidity sensor, Raindrop Sensor, DC step down module 12 volts to 7volts and 12 volts to 5 volts, 25A ESC, 4 Poles 4800 KV BLDC, 7-volt Power Supply, MG995 Servos for Steering.

Figure 3. Possible devices for Base Station.

3.2 Base Station Components

Figure 3 shows the possible base station components. They consist of any machine or device on any OS platform having modern browsers (IE10+, Chrome 16+, Firefox 11+, Safari 6+). In addition, they can run HTTP to become a WebSocket client to control the Robot when connected over standard Wi-Fi.
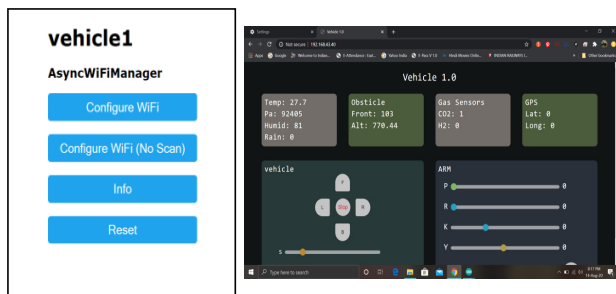
Figure 4. Login Page and Control Panel.

3.2.1 GUI

WebSocket in JavaScript and HTML5, CSS for webpage design runs only on present-day programs like IE10+, Chrome 16+, Firefox 11+, and Safari 6+. A website page that keeps up a WebSocket customer association with a WebSocket worker can frequently trade information by operating continuously and with low latency over a steady, full-duplex network. The method is used to implement a web-based GUI using JavaScript. A web socket server-based login page and control panel [8] is shown in Fig 4. This GUI assists operator with live distance from the vehicle to an obstacle in the front with altitude reading and GPS location. The car decelerates near the obstacle for safety, and it can be overridden by reviewing the situation. WebSocket server connects to the endpoint via a URL ws://126.25.3.1:8080/WebSocketServer/echo.

3.2.2 Object Detection and Assistance Program

To assist the user in low light, extremely bright, blur vision of FPV camera in surroundings, the program designed in Visual Studio renders the live feed with essential services like object detection, edge detection, and detecting the object's shape on the computer. Thus, it avoids the usage of an expensive graphics processor on the vehicle. Figure 5 shows the object detection user interface used for assistance.
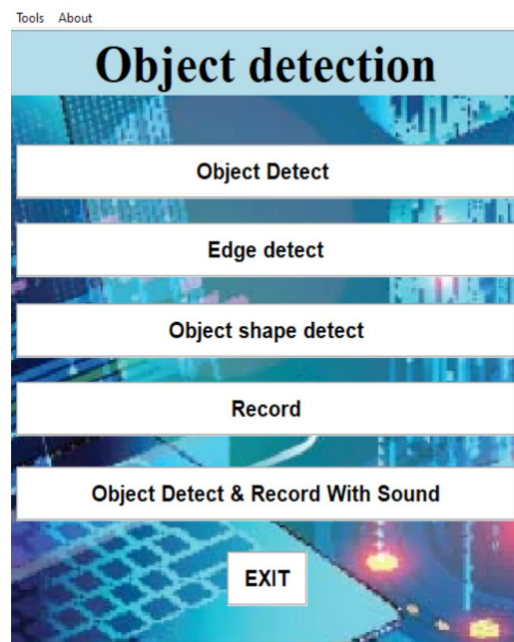
Figure 5. Program for Object detection for user assistance.

3.3 Software

The software used for the development of the Robot

include, Arduino IDE, XCTU, Autodesk Fusion 360, Cura 4.6, Auto CAD, 2020, Adobe XD, Visual Studio Code.

3.4 Design of Mechanical System

The design's first steps consisted of evaluating the existing Robot by analyzing the different operations and considering the available space for mounting the sensors, motors, and drivers. Then, the development of several design configurations was done and also evaluated. Finally, it led to the selection and implementation of optimal arrangement with the following criteria:

1) Robot modification should be minimal to bring back quickly to its initial state.
2) Modular system design should be adopted for easy maintenance.
3) Simple part configurations can bring down the cost of manufacturing.
4) Materials available locally should be used.
5) Automated control for deceleration.
6) Automated control of the steering.
7) Obstacle detection.
8) Easily travel on rough terrains.
9) Efficient use of the Camera.
10) It uses 7 V to supply all of the necessary power.
11) Robotic arm to perform simple tasks.
12) The Robot uses a sturdy and stable design to support all the other onboard components.
13) Study the environmental parameters.

3.4.1 Traversing capability till 45-degree inclination

A mechanical coupler [12] between two vehicle bodies gives adaptive motion providing adjustment to the body's total bend in a safe zone using limiters to have better traction over rough terrains. A servo for suspension allows adjustment to the body's complete bend to have better traction and maneuver over rough terrains. For instance, different robots have every one of the four wheels similar for a forward movement. If there should arise an occurrence of left or right turns, the wheels' speed should be eased back down or reversed depending on the velocity. To overcome the drawbacks, we intend to accomplish all the movements by keeping the wheels' speed the same and performing more extreme turns even at a higher rate by changing the wheels' speed.

3.4.2 Flexibility to twist and turn movements

Different robots will, in general, alter wheel speed or course to take turns. We intend to accomplish more extensive turns by having an articulation steering system with a mechanical differential. It doesn't affect motor rpm keep-

ing momentum reserved, which helps to decrease power consumption. Thus the overall range and average speed are increased while maintaining the necessary abilities fully functional.

3.4.3 Greater length to width ratio

The complete Robot is designed to have two hexagonal units, each of 20*20 cm, covering a total rectangular plane of 46*20 cm, which gives better stability and flexibility than other robots.

3.4.4 Environmental parameters and human assistance

The sensors are placed on the Robot to capture the ecological parameter readings. Sensors send information such as Hydrogen and Carbon monoxide concentration, co-fixations noticeable in the environment, and co-gas recognition in the range of 20 to 2000ppm. Further, they sense a reduction in the resistance in transmitter power due to raindrops in the environment and nearness of water interface nickel lines equal to the sensor, thus decreasing opposition and lessens voltage drop. It utilizes a capacitive humidity sensor and a thermistor to analyze surrounding air, hence sensing its temperature and humidity. The system's prime objective is to assist humans in critical circumstances where human life is a threat.

3.5 Forward Kinematics Equations

In this section, forward kinematics infers conditions for articulated steering vehicles. This type of vehicle comprises two separate wagons associated with an articulated joint in the center. Steering is achieved by exerting force (push or pull) on the wagon's edge closest to the central joint. Articulated vehicles are generally used as actual working vehicles, such as road rollers and various woodland or construction vehicles.
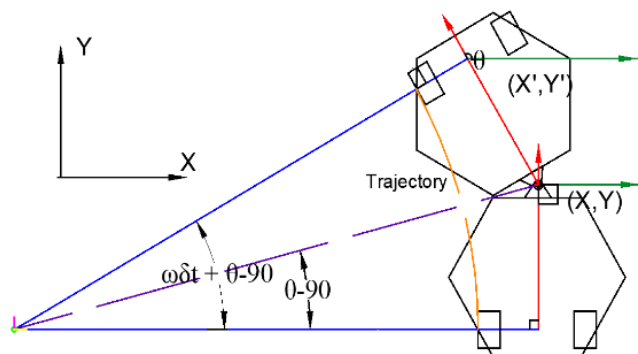

Figure 6. Articulated system.

All wheels move toward a path opposite its pivot while taking a turn with full contact on the ground to achieve

slip-free movement. The separation obtained can be processed using available data like the wheel diameter and its rotational speed. For some reason, this itself is a romanticized circumstance. Nevertheless, slip is regularly noteworthy and challenging to display. Thus, slip-free movement is regularly accepted when taking care of the issues expressed previously.

For a multi-axle vehicle, the axle axes' intersection point is known as the middle point for the turn when the vehicle maneuvers was proposed by Hellström et. al., [3]. This specific point is known as ICC, which means the Instantaneous Center of Curvature. It is also known as ICR, which means the Instantaneous Center of Rotation. As a rule, thoroughly slip-free movement isn't mathematically conceivable. The circumstance for this vehicle with three axes is outlined in Figure 6.

The shifting guiding edge φ, as shown in Figure 7, makes it challenging to develop the vehicle with the end goal that the axes meet at one point. A typical methodology accepts two virtual axes situated in the middle of the genuine axes in the vehicle's front and back to abstain from displaying slip. The external piece of a wheel travels in more drawn-out separation than the internal part in all bends. Subsequently, they might slip. Moreover, all wheels' velocities must be wholly controlled to achieve the end goal of slip-free movement in any event around conceivable. The furthest wheels need to pivot quicker than the deepest ones, and the back ones need to turn slower than the front ones (expecting a more drawn-out back part as in Figure 7). Contingent upon mechanical development and vehicle's control arrangement, this is a pretty much legitimate suspicion. The accompanying kinematics conditions are inferred with all previously mentioned glorified presumptions.
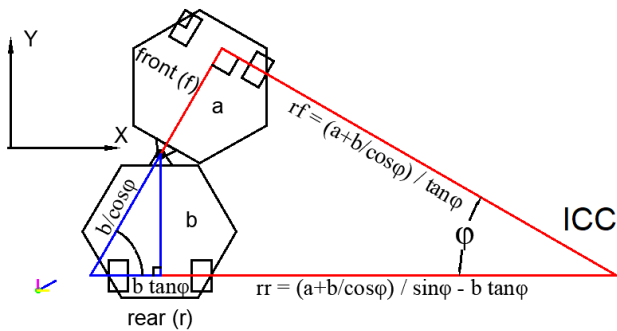
Figure7. Rotational radius of a vehicle with articulated steering of angle φ, front length as a, and rear length as b.

The distance from a circle (ICC) center to the end of either of the virtual axis is the radius with notation r. For an articulated vehicle, 'r' is derived using the vehicle's geometric equations and the steering angle, as illustrated in

Figure 7. For the front axis, radius rf is given by,

$$rf = (a + b/\cos\varphi) / \tan\varphi \qquad (1)$$

For the rear axis, radius rr is given by,

$$rr = (a + b/\cos\varphi) / \sin\varphi - b \tan\varphi. \qquad (2)$$

We can consider the forward portion of the vehicle's movement with an assumption of the above equations since the vehicle's calculation gives the rear part's indication. By taking an example where a vehicle present (x,y,θ) are estimated at the center of the virtual front pivot at time t to obtain (XICC, YICC) for ICC, the equation used is:

$$(XICC, YICC) = (x - r \sin\theta, y + r \cos\theta) \qquad (3)$$

where r for the straightforwardness of the reading list means the range rf.

A movement from the present (x,y,θ) at time t to present (x', y', θ') at time 't + δt' is represented in Figure 8. Since the vehicle moves along a circle, it might be useful to articulate the current speed 'ω,' characterized as 2π/T radians/second. T is the total time it would take to complete one complete pivot ICC. The realized vehicle speed v is thought to be the speed at which the front pivot moves (this is another presumption that could be appropriately verified). It would thus be able to be interpreted as 2πr/T that provides accompanying articulation for ω:

$$\omega = v/r. \qquad (4)$$

The new angle θ' at time t + δt can be given as

$$\theta' = \omega\delta t + \theta \qquad (5)$$
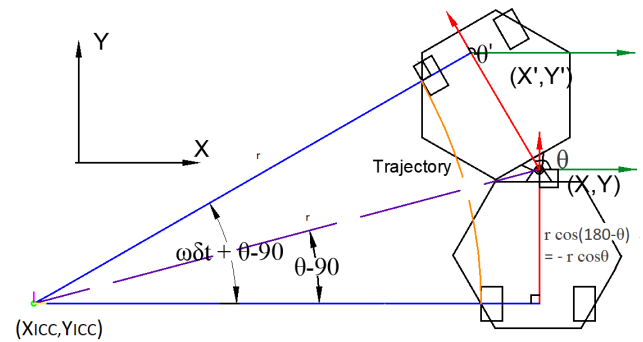
Figure 8. Rotation of vehicle around ICC with angle ωδt. Here position changes from (x,y,θ) to (x', y',θ') which is represented in a global coordinate system (top left). The ICC coordinates are $(x - r \sin\theta, y + r \cos\theta)$.

The new position (x',y') at time t + δt is registered by a two dimensional pivot of the point (x,y) by ωδt degrees around the point ICC:

$$x' = \cos(\omega\delta t)(x - XICC) - \sin(\omega\delta t)(y - YICC) + XICC \qquad (6)$$

$$y' = \sin(\omega\delta t)(x - XICC) + \cos(\omega\delta t)(y - YICC) + YICC. \qquad (7)$$

To sum up and come back to the first issue for the enunciated vehicle in Figure 8 an underlying posture (x,y,θ), a detailed vehicle speed v and a guiding point φ at time t, the posture (x',y',θ') at time t + δt can be assessed by the calculations (1) to (7). As referenced over, the introduction of the new posture makes a few presumptions:

1. Assuming a completely slip-free motion (ignoring geometrical difficulties, tires with width, the conflict between the front and rear-wheel speed, and other terrain conditions).

2. The deduction of the conditions utilizes two virtual wheel axes situated in the middle of the genuine wheel axes.

3. The velocity v is assumed to be the forward portion's speed. The vehicle's total assessed speed is calculated with the motor RPM and the transmission. This real speed is different from that of the forward portion's rate.

4. Results and Discussion

The proposed system includes an application that controls the development of the Robot. The implanted equipment is created on ESP-32 and managed based on Android, IOS, or Windows. ESP regulator is to get and takes the information and supervises the Robot engines using ESC. As a result, the Robot can push ahead, opposite, left, and right developments. Figure 9 (a) illustrates the UGV prototype. Wi-Fi module is inbuilt to receive commands. A remote camera is mounted on the robot body for security reasons.
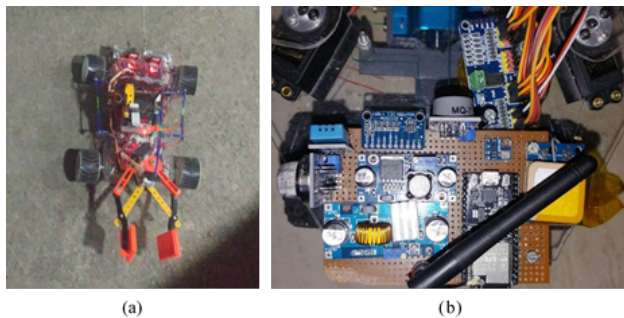
Figure 9. UGV (a) First prototype of the mechanical system for UGV. (b) Its main control boards.

Tele operation is achieved using a web-based GUI on any machine connected to standard Wi-Fi. The base station trans receives a request via a hypertext transfer protocol using a web socket. At the beneficiary end, these orders are utilized for controlling the Robot. Main control board Figure 9 (b) highlights the hardware components used in UGV. The circuit board consists of various sensors, voltage regulators, Microprocessor, a GPS module, an ADC chip, PWM driver controllers to control the Robot.

4.1 Preliminary Test
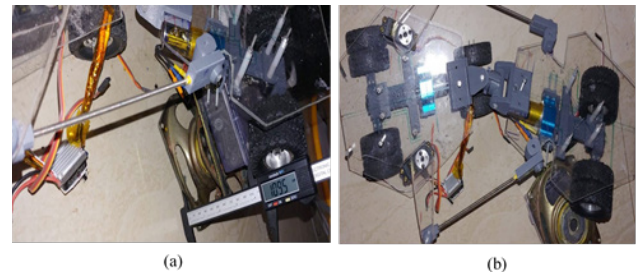
Figure 10. Vehicle body (a) Total height from ground the front body can be raised keeping the rear body intact. (b) Rotating movement.

The ground's height provides a [12] twisting and lifting or lowering angle of 33 degrees. Figure 10 (a) shows raised the height of the body from the ground. Thus, the maximum lowering or raising pitch is 33 degrees for each body. Suppose the Robot is taken on a graph paper vertically aligned on the y axis. The front end and rear end are parallel to the y axis. Then, the front or rear body can freely rotate around the y-axis, keeping the other body's angle intact [9]. The maximum twisting angle is 55 degrees. The rotating movement is demonstrated in Figure 10 (b). The communication between the base station and Robot over the Wi-Fi network minimizes a full-duplex connection.

Figure 11. Robotic arm and UGV (a) Robotic arm with 5 degrees of freedom [6] used for assistance in critical circumstances (b) Unmanned vehicle carrying drugs for contactless delivery.

The development of adaptive traction gives the Robot the ability to maneuver over any terrain. Applications like surveillance, medicine, and equipment delivery systems assist humans in critical circumstances with a Robotic arm. A robotic arm with a freedom of 5 degrees helps in vital cases, as illustrated in Figure 11 (a). Figure 11(b) shows the UGV employed for contactless drug delivery.

4.2 Vehicles Design Validation

Figure 12 (a) shows our vehicle's adaptive pitch positions at different climb angles from the ground to the surface, and Figure 12 (b) highlights the adaptive roll positions between the front and read the body.
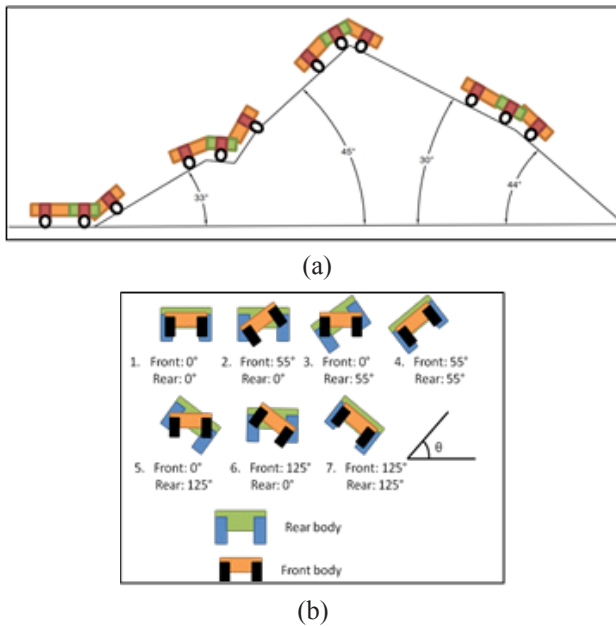
Figure 12. Moving vehicle pitch positions (a) Adaptive pitch in different positions (b) Adaptive Roll positions.

Similarly, a plot in Figure 13 (a) describes the vehicle's adaptive pitch angles of the front, mid, and rear axles during movement. The plot in Figure 13 (b) depicts the vehicle's adaptive roll angles of the front and rear axles. The constructed Robotic arms can is an independent wanderer fit for remote controlling applications. We have added the rotating Camera on this arm to view objects and control the path easily. We achieved obstacle detection and boundary detection to differentiate the objects for real-time tracking and GPS. Our proposed UGV provides current correspondence headway administrations to give simple and easy mobility [4,5,10,11]. The contactless drug delivery UGV can easily be deployed in COVID-19 hospital wards, as demonstrated in Figure 11 (b).
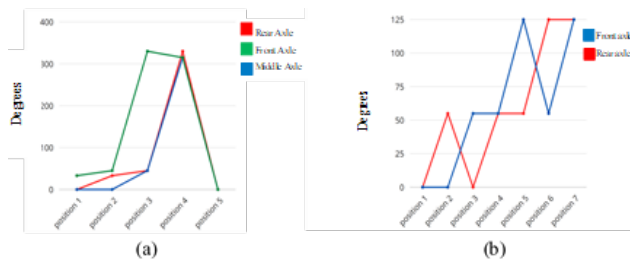
Figure 13. Vehicle pitch angles between axles (a) Adaptive pitch angle compared between all axles (b) Adaptive roll angle compared with front and rear axle.

5. Conclusions and Future Scope

The fusion of UGV technologies has given us the way to accomplish objectives that have never been acknowl-edged in such a productive way before. These advancements achieve a self-dependant and capable machine to handle Situations all alone and facilitate a human's activity in current situations. The vehicle assembling, configuration, and controlling abilities of a designer play an essential role in developing more complex UGV applications. The proposed UGV design provides the following advantages,

- The UGV can turn at extreme speeds or during climb without changing motor rpm and without losing traction.
- Utilize independent motors for wheels. It can maneuver using two 7V BLDC and two 7V SERVO with total continuous consumption of 2A current and the max peak of 4A while pulling 5-6Kg of load. As a result, the UGV is efficient and consumes less power.
- The hexagonal body, unlike other controlled vehicles, increases usable space onboard with a reduction of weight. In addition, the unique adaptive pitch and roll give excellent traction and maneuverability over any terrain.
- It provides an automatic deceleration safety feature in obstacle detection and null reading in case detection of edge cliff. However, this function can override user input after reviewing as this vehicle can climb most of the obstacles like stairs, riverbank, and elevated footpath. The vehicle can also be located in real-time via GPS positioning.
- The drive-train is not back-drivable, making vehicle and motor stay idle when need to stop on slopes without consuming any extra power.
- The body has fewer connecting and simple parts. As a result, the whole vehicle never fails at once, and any failed part can easily be replaced.

The proposed UGV has the following limitations,

- The system assists the operator in navigation, and the vehicle is semi-autonomous.
- The adaptive body motion has to be changed to an active state manually.
- Most of the parts are fabricated using additive manufacturing, and the surface becomes brittle over time.

The proposed model can be improved by making the vehicle completely autonomous. The vehicle's navigation system can be enhanced by using the waypoints method. The vehicle's robustness can be improved by building the body using carbon fibers. The proposed model can be further be improved by optimizing the battery power and testing load-carrying capacities after integrating solar power. The conversion of this prototype to full-scale UGV will be helpful in many situations similar to today's pandemic COVID-19.

References

[1] F. Le Menn, P. Bidaud and F. Ben Amar, "Generic differential kinematic modeling of articulated multi-monocycle mobile robots," Proceedings 2006 IEEE International Conference on Robotics and Automation, 2006. ICRA 2006., Orlando, FL, USA, pp. 1505-1510, 2006.
DOI: 10.1109/ROBOT.2006.1641921.

[2] Valjaots, Eero, and Raivo Sell. "Energy efficiency profiles for unmanned ground vehicles/Energiaefektiivsuse profiilid mehitamata soidukitele." Proceedings of the Estonian Academy of Sciences, vol. 68, no. 1, pp. 55 onwards, 2019.

[3] Hellström, Thomas, Kinematics equations for differential drive and articulated steering, Department of Computing Science, Umeå University, Book, 2011.

[4] Tavakoli, Mahdi, Jay Carriere, and Ali Torabi, "Robotics, smart wearable technologies, and autonomous intelligent systems for healthcare during the COVID-19 pandemic: An analysis of the state of the art and future vision," Advanced Intelligent Systems 2.7, Article, Issue 6, 2020.
DOI: 10.1002/aisy.202000071.

[5] Khan, Zeashan Hameed, Afifa Siddique, and Chang Won Lee. "Robotics utilization for healthcare digitization in global COVID-19 management." International journal of environmental research and public health 17.11 Article, Issue 5, 2020.
DOI: 10.3390/ijerph17113819.

[6] V.N. Iliukhin, K.B. Mitkovskii, D.A. Bizyanova, A.A. Akopyan, "The Modeling of Inverse Kinematics for 5 DOF Manipulator," Procedia Engineering, Volume 176, pp. 498-505, 2017.

[7] Jean-Luc PAILLAT, Philippe LUCIDARME, Laurent HARDOUIN, "Evolutionnary stair climbing controler for Unmanned Ground Vehicles," IFAC Proceedings Volumes, Volume 42, Issue 16, pp. 131-136, 2009.

[8] Lakshminarasimhan Srinivasan, Julian Scharnagl, Klaus Schilling, "Analysis of WebSockets as the New Age Protocol for Remote Robot Tele-operation," IFAC Proceedings Volumes, Volume 46, Issue 29, pp. 83-88, 2013.

[9] Merlin Morlock, Niklas Meyer, Marc-André Pick, Robert Seifried, "Real-time trajectory tracking control of a parallel robot with flexible links," Mechanism and Machine Theory, Volume 158, 2021.

[10] Lakshminarasimhan Srinivasan, Julian Scharnagl, Zhihao Xu, Nicolas Faerber, Dinesh K. Babu, Klaus Schilling, "Design and Development of a Robotic Teleoperation System using Duplex WebSockets suitable for Variable Bandwidth Networks," IFAC Proceedings Volumes, Volume 46, Issue 29, 2013.

[11] Vu Phi Tran, Matthew A. Garratt, Ian R. Petersen, "Multi-vehicle formation control and obstacle avoidance using negative-imaginary systems theory," IFAC Journal of Systems and Control, Volume 15, 2021.

[12] Lingfei Qi, Tingsheng Zhang, Kai Xu, Hongye Pan, Zutao Zhang, Yanping Yuan, "A novel terrain adaptive omni-directional unmanned ground vehicle for undeground space emergency: Design, modeling and tests," Sustainable Cities and Society, Volume 65, 2021.

ARTICLE
Student Performance Prediction Using A Cascaded Bi-level Feature Selection Approach

Wokili Abdullahi[1]   **Mary Ogbuka Kenneth**[1*]   **Morufu Olalere**[2]

1. Department of Computer Science, Federal University of Technology, Minna, Nigeria
2. Department of Cyber Security Science, Federal University of Technology, Minna, Nigeria

ABSTRACT

Features in educational data are ambiguous which leads to noisy features and curse of dimensionality problems. These problems are solved via feature selection. There are existing models for features selection. These models were created using either a single-level embedded, wrapper-based or filter-based methods. However single-level filter-based methods ignore feature dependencies and ignore the interaction with the classifier. The embedded and wrapper based feature selection methods interact with the classifier, but they can only select the optimal subset for a particular classifier. So their selected features may be worse for other classifiers. Hence this research proposes a robust Cascade Bi-Level (CBL) feature selection technique for student performance prediction that will minimize the limitations of using a single-level technique. The proposed CBL feature selection technique consists of the Relief technique at first-level and the Particle Swarm Optimization (PSO) at the second-level. The proposed technique was evaluated using the UCI student performance dataset. In comparison with the performance of the single-level feature selection technique the proposed technique achieved an accuracy of 94.94% which was better than the values achieved by the single-level PSO with an accuracy of 93.67% for the binary classification task. These results show that CBL can effectively predict student performance.

1. Introduction

The role of education in the development of any country cannot be over emphasised. This is because of its' impacts on the social, economic and political developments in any society [1]. The quality of any nation is directly proportional to the quality of her education system, hence, the ongoing efforts to improve the quality of educational institutions. Academic performance of students in any educational institution is a measure of the institutions efficiency in knowledge delivery [2].

The interest of researchers and scholars on learning outcomes have grown exponentially and this account for the reason why scholars have been working hard to find out factors that affects good academic performance [1]. There are different factors that affects students' performance. They include: intelligence, state of health, motivation, anxiety, suitable learning environment, adequate education infrastructures, family and parental influences, societal influences, institutional influences [3].

In Computer Science, one of the active fields is data mining. Data mining deals with the process of extracting

---

Corresponding Author:
Mary Ogbuka Kenneth,
Department of Computer Science, Federal University of Technology, Minna, Nigeria;
Email: Kenneth.pg918157@st.futminna.edu.ng

valuable information from raw data [4]. Data mining is crucial due to the rising amount of data and the immediate need to translate these data into practical information. Presently, data mining technique is being applied to different sectors of life. The educational sector is a significant area in which data mining is gaining increasing interest. In educational field data mining is referred to as Educational Data Mining (EDM). EDM emphasizes that useful knowledge is obtained from educational information systems such as the course management systems, registration systems, online learning management systems, and application systems. Predicting the academic success of students is a significant application of EDM. In the educational environment, the analysis and estimation of student performance is an integral aspect. This prediction task foresees the importance of an unknown variable that distinguishes students with outcomes such as pass or failure, grades and marks [5].

EDM emerges as a result of rapid growth in educational data and this has presented several challenges to researchers to develop more efficient data mining methods [6]. In EDM the features in educational data are ambiguous which leads to the curse of dimensionality problem. This issue of curse of dimensionality and noisy features can be solved using dimensionality reduction. Dimensionality reduction can be achieved via feature selection. The purpose of feature selection is to select an appropriate subset of features which can efficiently describe the input data, which reduces the dimensionality of feature space and removes irrelevant data. There are existing models for selection of student performance features. However these models were created using either a single-level embedded, wrapper-based or filter-based methods. Filter methods are fast and independent of the classifier but ignore the feature dependencies and also ignores the interaction with the classifier [7]. Since both embedded and wrapper based feature selection methods interact with the classifier, they can only select the optimal subset for a particular classifier. So the features selected by them may be worse for other classifiers [8,9]. Filter-based method is fit for dealing with data that has large amounts of features since it has a good generalization ability. Given the importance of features and the relevance between features, the filter-based feature selection algorithm can only rank the features and cannot optimally select the subset of the selected features. Therefore, particle swarm optimization was used to optimally select the subset of the selected features after performing filter-based selection. Hence, this research work proposes a cascaded bi-level feature selection approach to overcome the drawbacks of a single filter-based and wrapper-based selection techniques for student performance

prediction. The contributions of this study are:

(1) Development of a cascaded bi-level feature selection technique for student performance prediction.

(2) Selection of optimal features using the cascaded bi-level feature selection technique.

(3) Evaluation of performance of the cascaded bi-level feature selection technique.

The following is how the rest of the paper is structured: A summary of related researches on student performance prediction is included in section two. The techniques used to accomplish the goal of student performance prediction is presented in section three. In section four results from the experimentation are presented and discussed. The study's conclusion is presented in section five and lastly future works are presented in section six.

2. Related Works

Students' viability of progress is essential to predict student performance. The significance of predicting student performance has led researchers to become more and more interested in this field. Therefore, various researches have been published to predict students' performance.

In the study by Lau [10] ANN was used to evaluate and predict the students' CGPA using the data about their socio-economic background and entrance examination results of the undergraduate students from a Chinese university. In order to evaluate the performance of ANN, computations of Mean Square Error (MSE), regression analysis, error histogram and confusion matrix are introduced to ensure the appropriateness of ANN's performance in mitigating the arising of over fitting issues. Overall, the ANN has achieved a prediction accuracy of 84.8%, and with AUC value of 0.86. However the proposed Artificial Neural Network (ANN) method performs poorly in classifications of students according to their gender, as high False Negative rates are obtained as results, which is likely due to high imbalance ratio of two different types of sample.

Olalekan [11] adapted Bayes' theorem and ANN to construct a predictive model for students' graduation probability at a tertiary institution. Four variables were used for prediction: Unified Tertiary Matriculation Test, Number of Sessions at the high school level, Grade Points at the high school level and Entry Mode. The data used was collected from the Computer Science School, Federal Polytechnic, Ile-Oluji, in Ondo State, Nigeria. The data were composed of 44 examples with five attributes. The study concludes that the ANN has a 79.31% higher performance accuracy than the 77.14% obtained by the Bayes classification model. The ANN precision improved as the hidden layers increased. As compared to other previous works, the overall accuracy in this study was low because of the small size

of data used. Expanding the data size would help enhance the accuracy of the classification of the model.

Salal [12] presented a model for student performance classification based on the Eurostat Portuguese data set consisting of 33 attributes and 649 instances. Nine classifiers namely: ZeroR, Naïve Bayes, Random Forest, Random Tree, Decision Tree (J48), REPTree, Simple Logistic, JRip, and OneR were utilized in this study. In this study feature selection was performance using filter-based technique. All the nine classifiers had performance improvement when trained with the selected features. For instance the decision tree classifier with an accuracy of 67.79% when trained with all the feature attained 76.27% when trained with the selected features. This shows that student's attributes affect the student performance. The drawback of the proposed system is that filter-based feature selection techniques ignore the feature dependencies and also ignore the interaction with the classifier.

Magbag and Raga [13] focused on building a model to predict first-year students' academic success in tertiary education. This research aimed to allow early intervention to help students stay on course and reduce non-continuance. The data utilized in this paper were obtained from three higher education institutions in Central Luzon, primarily in the cities of Angeles, San Fernando and Olongapo. The study subjects included first-year students from 8 academic departments from 2018-2019; Arts and Sciences, Engineering and Architecture, Computer Studies, Criminology, Education, Hospitality and Tourism, Business and Accountancy, Nursing and Allied Medical Sciences. The dataset was composed of 4,762 examples. The dataset was pre-processed, and missing values were deleted, leaving 3,466 available samples. Using Correlation-based Feature Selection, Gain Ratio and Information Gain for feature rating, feature selection was carried out. Using these selected features, the NN and logistic regression models were trained and evaluated. In comparison with similar works, the scale of the dataset used rendered the scheme more robust. However, the accuracy of 76% achieved in this analysis is low.

Ünal [14] performed student performance prediction using feature selection. Decision tree, random forest and Naïve Bayes were employed on the educational datasets to predict the final grades of students. In this study two experiments were conducted. The first experiment deals with training the classifiers without feature selection. And the second experiment deals with training the classifiers after feature selection. In the second experiment wrapper feature selection technique was used to select the most relevant feature set, while the irrelevant features were removed. The second experimentation produced an improved accuracy due to the applied feature selection than

the first experiment without feature selection. For instance the accuracy of Naïve Bayes improved from 67.80% in the first experiment to 74.88% in the second experiment. The EuroStat dataset from secondary education of two Portuguese schools were used. This issue with the feature selection technique used in this study is that they are classifier dependent. That is a set of features selected by a particular classifier and works well for that classifiers. Those not mean those set of features will also perform well for other classifiers/models.

3. Methodology

This section presents the research methods that were followed in the study. It provides information on the dataset, data encoding method, feature selection and data classification. The diagram presenting each of the method used for student performance prediction is presented in Figure 1.
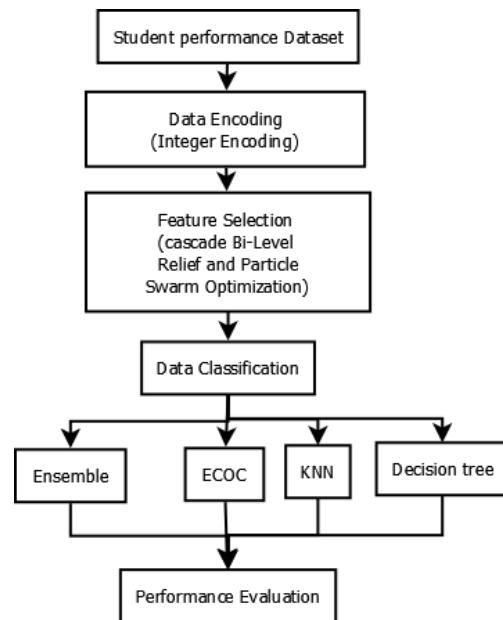
Figure 1. Proposed System

3.1 Dataset

This study's dataset is known as the student performance dataset. The data were obtained from the University of California at Irvine's repository. The student performance data were collected from two public schools in the Alentejo region of Portugal during the 2005-2006 academic year. The dataset consists of secondary school accomplishment statistics from two Portuguese schools. The data were acquired through school reports and surveys and include student grades, demographic, social, and school-related characteristics. Two datasets are provided, one for mathematics and the other for Portuguese lan-

guage performance. The mathematics data set consist of 395 instances and 33 attributes where 32 attributes are the predictors while one attribute (attribute 33) is the target. The Portuguese data set consist of 649 instances with 33 attributes. In Cortez and Silva [15], the two datasets were modeled under binary and five-level classification tasks. These two classification task is explained in section 3.2.

3.2 Data Preprocessing

The overall assessment in the original data, as in several other countries, is on a scale of 0-20, with 0 being the worst and 20 being the best. Because the students' final score is in the form of integers, and the predicted class should be in the form of categorical values, the data had to be transformed to categories according to a scoring policy. Two separate grading systems were employed in this study: binary grading and five-level grading. First, the final grade was divided into five categories. These ranges are described using the Erasmus framework. The scale 0-9 equates to grade F, which is the lowest grade and corresponds to the mark "fail". The remaining class labels (10-11, 12-13, 14-15, and 16-20) correspond to D (sufficient), C (satisfactory), B (good), and A (excellent) respectively. Secondly, the final grade was categorized into two (binary) categories: fail and pass. Table 1 shows the five-level grading categories. The binary-level grading categories are shown in Table 2. In Table 2, the range of 0-9 corresponds to F, and it means "fail"; the range of 10-20 refers to A, B, C, and D, and it means "pass."

Table 1. Five-level grading categories

1	2	3	4	5
Excellent	Good	Satisfactory	Sufficient	Fail
16-20	14-15	12-13	10-11	0-9
A	B	C	D	F

Table 2. Binary-level grading categories

0	1
Fail	Pass
0-9	10-20
F	A, B, C, D

3.3 Data Encoding

There are both numeric variables and categorical variables

in the dataset used. Categorical variables are usually represented as 'strings' or 'categories' and are finite in number. In this phase, the categorical data types of attributes were converted to numeric attributes. Data encoding was done because specific machine learning algorithms such as Naïve Bayes, support vector machine and Ensemble need numeric attribute types to work. The integer encoding technique was employed in this research. Integer encoding involves mapping each string attribute to an integer value. Integer encoding was used for the categorical (string) class because the integer values have a natural ordered relationship between each other and machine learning algorithms may be able to understand and harness this relationship. And the categorical attributes has an order relationship [16]. Table 3 indicate gender representation after integer encoding.

Table 3. Integer encoding for Gender Attribute

Male	1
Female	2

3.4 Feature Selection

Feature selection is a process that selects pertinent features as a subset of original features [17]. In real-world situations, relevant features are often unknown a priori. Hence feature selection is a must to identify and remove the irrelevant/redundant features for student performance prediction [18]. This paper proposed a novel cascade bi-level feature selection approach for the classification of student performance data, which used filtering technique such as Relief (RF) and optimization technique such as Particle swarm Optimization (PSO).

The proposed method is divided into two levels. In the first level (level 1) the Relief technique was used to select 20 sets of features based their shared information. The selected 20 sets of features were gathered and a new feature subset is generated. In the second level (level 2) the new 20 feature subset is used as input to the PSO and an optimized feature subset is selected. The proposed feature selection scheme is presented in Figure 2.

3.4.1 Relief Feature Selection Technique

Relief is a feature selection algorithm that uses a filter-method approach that is particularly sensitive to feature interactions.
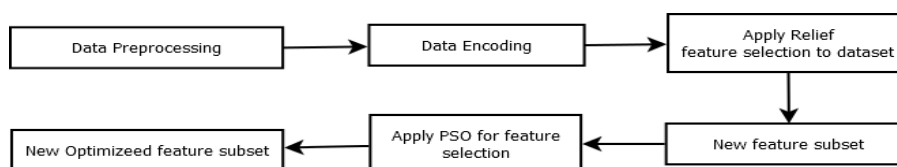

Figure 2. Proposed feature selection technique

Relief calculates a proxy statistic for each feature that can be used to measure feature 'quality' or 'relevance' to the target definition [19]. These feature statistics are known as feature weights (W [A] = weight of feature 'A') or feature 'scores,' and they can vary from -1 (worst) to +1 (best).

The advantages of using the Relief method is that it is computational fast even when there is a big amount of data. Time complexity is not a problem because a consistent number of trials is completed. As a result, the relief technique may complete faster than other filter-based approaches that require all of the data to be considered [20].

Given the importance of features and the relevance between features, Relief filter-based selection feature algorithm selects relevant feature based on their relationship with dependent variable however in Relief method the interaction with the classifier and each feature is considered independently thus ignoring feature dependencies. To enable feature dependencies and classifier interaction, the particle swarm optimization is used to optimally select a subset from the selected features.

3.4.2 Particle Swarm Optimization (PSO)

Particle swarm optimization (PSO) is a computational technique for solving problems by iteratively trying to enhance a candidate solution in terms of a quality metric [21]. It solves a problem by generating a population of possible solutions, which are referred to as particles, and moving them around in the search space using a simple mathematical formula based on their position and velocity [22]. Consider the global optimum of m-dimensional function defined in Equation 1.

$$G(x_1, x_2, x_3, x_4, ..., x_m) = G(X) \tag{1}$$

Where x_i is the search variable, which represents the set of free variables of the given function. The aim is to find a value x^* such that the function $G(x^*)$ is either a maximum or a minimum in the search space. The PSO algorithm is a multi-agent concurrent search method in which each particle represents a potential solution in the swarm. All particles go through a multidimensional search space, where each particle adjusts its position based on its own and neighbouring experiences (Poli et al., 2007 Suppose x_i^s denotes the position vector of particle I in the multidimensional search space at time step s, then Equation 2 is used to update the position of each particle in the search space.

$$x_i^{s+1} = x_i^s + v_i^{s+1} \ with \ x_i^0 \sim U(x_{min}, x_{max}) \tag{2}$$

Where v_i^s is the velocity vector of particle I that drives the optimization process and reflects both the own experience knowledge and the social experience knowledge from the all particles. $U(x_{min}, x_{max})$ is the uniform distri-

bution where x_{min} and x_{max} are its minimum and maximum values respectively.

The velocity of the particle i updated using Equation 3.

$$v_i^{s+1} = w * v_i^s + c_1 * r_{1i} * (p_i - x_i^s) + \\ c_2 * r_{2i} * (p_g - x_i^s) \tag{3}$$

Where s denotes the sth iteration in the process, w is inertia weight and c_1 and c_2 are acceleration constants. r_{1i} and r_{2i} are random values uniformly distributed in [0,1]. p_i and p_g represent the elements of $pbest$ and $gbest$ respectively. The flowchart for selection of features using PSO is shown in Figure 3.
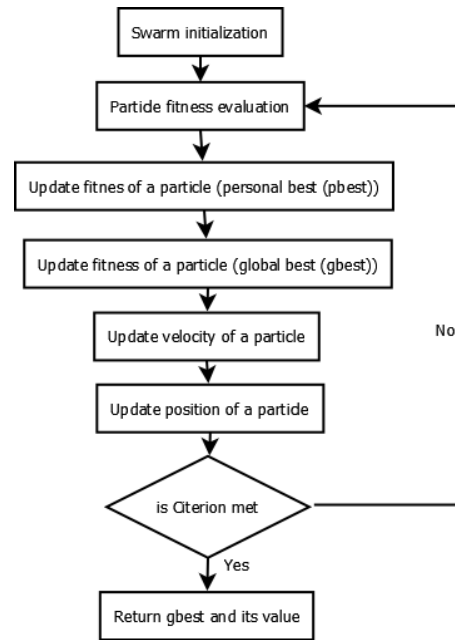
Figure 3. Flow chat for PSO feature selection

Therefore, in a PSO method, all particles are initiated randomly and evaluated to compute fitness together with finding the personal best (best value of each particle) and global best (best value of particle in the entire swarm). After that a loop starts to find an optimum solution. In the loop, first the particles' velocity is updated by the personal and global bests, and then each particle's position is updated by the current velocity. The loop is ended with a stopping criterion predetermined in advance [23].

3.5 Data Classification

In this research four machine learning classification models were used for training and classification: Error-Correcting Output Codes (ECOC), Decision Tree (DT), Ensemble, and K-Nearest Neighbor (KNN).

3.5.1 Error-Correcting Output Codes (ECOC)

The ECOC technique is a tool that allows the issue of multiclass classification to be interpreted as multiple problems of binary type, enabling the direct use of native binary classification models [24]. ECOC designs are independent of the classifier depending on the implementation. ECOC has error-correcting properties and has shown that the learning algorithm's bias and variance can be decreased [25].

3.5.2 Decision Tree (DT)

A decision tree is a supervised learning model in which data is continually separated based on a specific parameter. The decision tree employs a tree-like structure to progress from observations about an item (represented by the branches) to inferences about the item's target value (defined in the leaves) (Kolo *et al.*, 2015). Entropy is a popular technique used in determining which attribute to position at the root or the different levels of the tree [26]. Entropy is a measure of randomness in processed information [26]. The larger the entropy, the more challenging it is to draw any conclusions from that data. A branch with an entropy of zero, for example, is chosen as the root node, and further division is required for a branch with an entropy greater than zero [27]a novel concept of a non-probabilistic novelty detection measure, based on a multi-scale quantification of unusually large learning efforts of machine learning systems, was introduced as learning entropy (LE. In Equation 4, entropy for a single attribute is expressed.

$$E(S) = \sum_{i=1}^{n} - p_i log_2 p_i \tag{4}$$

Where S represents the present state, p_i is the probability of an event i of state S.

3.5.3 K-Nearest Neighour (KNN)

This is among the simplest machine learning model [28]. An item is classified based on its "distance" from its neighbours, and it is allocated to the most common class of its k closest neighbours [29,30]. The Euclidean distance is a linear distance between two points in Euclidean space [31]. If two vectors x_i and x_j are given where $x_i = (x_{i1}, x_{i2}, ..., x_{in})$ and $x_j = (x_{j1}, x_{j2}, ..., x_{jn})$, Then the Euclidean distance between x_i and x_j is given in Equation 5:

$$ED(x_i, x_j) = \sqrt{\sum_{k=1}^{n} (x_{ik} - x_{jk})^2} \tag{5}$$

3.5.4 Ensemble Classifier

An ensemble learning model combines predictions from multiple models with a two-fold goal: the first ob-

jective is to maximize prediction accuracy compared to a single classifier [32]. The second gain is more critical generalizability due to multiple advanced classifiers. As a result, solutions, where a single prediction model would have problems, can be discovered by an ensemble. A key rationale is that an ensemble can select a set of hypotheses out of a much larger hypothesis space and combine their predictions into one [33]. Via voting or weighted voting of their forecast for the final estimates, classifiers in the ensemble learning model are merged into meta-classifiers [34].

3.6 Performance Metrics

In this study, the accuracy, precision, recall, and f-score performance measures were used to evaluate the proposed method. This measure is explained below.

3.6.1 Accuracy

The rate of correct classifications is used to define accuracy. This is the number of correct guesses divided by the total number of right forecasts. The exact formula is given in Equation 6:

Accuracy=

$$\frac{True\ Positive + True\ negative}{True\ Positive + True\ negative + False\ Positive + False\ negative} \tag{6}$$

3.6.2 Precision

Precision is a metric used to calculate how many positive predictions are accurately made. The number of true positive elements is derived by dividing the total number of true positives by the total number of false positives. The formula in equation is used to define precision 7:

$$Precision = \frac{True\ Positives}{True\ Positives + False\ Positives} \tag{7}$$

3.6.3 Recall

Sensitivity is another term for recall. The amount of correct positive predictions that could have been made from all positive predictions is calculated by recall. The recall is calculated using the formula in Equation 8.

$$Recall = \frac{True\ Positives}{True\ Positives + False\ Negatives} \tag{8}$$

3.6.4 F-Score

The f-score of a model is defined as the harmonic average of recall and precision. F-Score is represented in Equation 9.

$$F - Score = 2 * \frac{precision * recall}{precision + recall} \tag{9}$$

4. Results and Discussion

In this work two classification tasks were carried out. These classification tasks are: binary-level grading classification and the five-level grading classification task. The Mathematics and the Portuguese dataset was used. The mathematics data set consist of 395 instances and 33 attributes while the Portuguese data set consist of 649 instances with 33 attributes. The datasets were divided in the ratio of 4:1 for training and testing (80% for training and 20% for testing).

4.1 Binary-level Grading Classification

The binary classification deals with classification using the two classes which are pass and fail. The dataset original label consist of 0-20 labels or grades. Where 0 is the worst grade and 20 is the best score. In the binary classification the integer labels were categorized into two classes where Fail (0) represents grade 0-9 and Pass (1) represents grade 10-20. Using the binary labels the four classifiers (ECOC, Ensemble, KNN and Decision Tree) were trained and tested using the original features (no feature selection done), sub-features using relief feature selector, sub-features using PSO feature selector and sub-features using the cascade bi-level feature selector. Table 4 presents the accuracy, precision, recall and f-score of all the four classifiers when trained with the original 32 features.

From Table 4 it can be seen that ensemble classifier performed best for Mathematics dataset with accuracies of 91.14%, f-score of 85.52%, precision of 77.38% and recall of 86.10% when compared with ECOC, KNN and DT. While KNN performed least with an accuracy

of 70.89%, f-score of 54.90%, precision of 43.75% and recall of 73.68%. For Portuguese dataset ECOC and Ensemble achieved same accuracy of 81.25% which presents them as the best performer. Table 5 presents the accuracy, precision, recall and f-score of all the four classifiers when trained with the Relief selected sub-features.

To properly evaluate the performance of ECOC, Ensemble, DT and KNN classifiers when trained with Relief selected feature subsets for both Mathematics and Portuguese data set, their precision, recall, f-score and accuracy are presented in Table 5. The ensemble classifier performed best with an accuracy of 92.41% and f-score of 86.35% for Mathematics dataset. While ECOC performed best with an accuracy of 93.08% and f-score of 82.35% for Portuguese dataset. Table 6 presents the accuracy, precision, recall and f-score of all the four classifiers when trained with the PSO selected sub-features.

In Table 6 Ensemble classifier obtained the best performance for both Mathematics and Portuguese data sets with an accuracy of 93.67% and an f-score of 87.90% for Mathematics data set and an accuracy of 94.62% and an f-score of 82.05% for Portuguese data set. ECOC, KNN and DT performance equally when trained with PSO selected Mathematics sub-features. However for the Portuguese data set KNN performed least with an accuracy of 91.42% and f-score of 70.59%.

A comparison of the classification results of the four classifiers for the original feature sets, relief feature set, PSO selected features and the cascade bi-level feature sets are shown Table 7.

In Table 7 an accuracy of 91.14% was obtained for Mathematics dataset classification using the original

Table 4. Binary-level classification results before feature selection

Before Feature Selection Classification Results							
	Mathematics				Portuguese		
Classifiers	Accuracy (%)	F-Score (%)	Precision (%)	Recall (%)	Accuracy (%)	F-Score (%)	Precision (%)	Recall (%)
ECOC	89.87	83.24	88.75	78.33	92.31	81.25	79.67	83.10
Ensemble	91.14	85.52	77.38	86.10	92.31	81.25	79.67	83.10
KNN	70.89	54.90	43.75	73.68	89.23	77.55	73.08	82.61
DT	87.34	77.76	70.00	87.31	91.54	77.06	80.51	84.35

Table 5. Binary-level Classification Results for Relief Selected Features

Relief Selected Features Classification Results							
	Mathematics				Portuguese		
Classifiers	Accuracy (%)	F-Score (%)	Precision (%)	Recall (%)	Accuracy (%)	F-Score (%)	Precision (%)	Recall (%)
ECOC	91.14	85.71	87.50	84.00	93.08	82.35	80.77	84.00
Ensemble	92.41	86.35	79.71	95.00	93.08	81.63	76.92	86.96
KNN	79.75	66.67	66.67	66.67	91.54	77.55	73.08	82.61
DT	89.87	82.61	79.17	86.36	92.31	79.17	82.61	86.36

Table 6. Binary-level Classification for PSO Selected Features

	PSO Selected Features Classification Results							
	Mathematics				Portuguese			
Classifiers	Accuracy (%)	F-Score (%)	Precision (%)	Recall (%)	Accuracy (%)	F-Score (%)	Precision (%)	Recall (%)
ECOC	92.41	84.21	76.19	94.12	93.85	78.95	75.00	83.33
Ensemble	93.67	87.90	85.71	90.00	94.62	82.05	80.00	84.21
KNN	92.41	84.21	76.19	94.12	91.42	70.59	60.00	85.71
DT	92.41	84.21	76.19	94.12	93.85	78.95	75.00	83.33

Table 7. Comparison of Feature Selection Techniques for Binary-level Classification Task

	Accuracy (%)							
	Mathematics				Portuguese			
Feature Selection	ECOC	Ensemble	KNN	DT	ECOC	Ensemble	KNN	DT
Before Feature Selection	89.87	91.14	70.89	87.34	92.31	92.31	89.23	91.54
Relief	91.14	92.41	79.75	89.87	93.08	93.08	91.54	92.31
PSO	92.41	93.67	92.41	92.41	93.85	94.62	91.42	93.85
Cascaded Bi-level	93.67	94.94	92.89	92.89	95.38	96.15	93.85	93.85

feature sets. While the original Portuguese dataset obtained the highest accuracy of 92.31% when trained with ECOC and Ensemble classifier. The highest classification accuracy obtained using the Relief selected features for the Mathematics data set is 92.41%. The PSO selected sub-features obtained a classification accuracy of up to 93.67% for the Mathematics data set. The proposed cascaded bi-level obtained a classification accuracy of 94.94% for the Mathematics data set. For the Portuguese data set the highest classification accuracy obtained for classification using the Relief selected features is 93.08% by Ensemble and ECOC classifiers. The PSO selected sub-features obtained a classification accuracy of up to 94.62% for the Portuguese data set. The proposed cascaded bi-level obtained a classification accuracy of 96.15% for the Portuguese data set. In conclusion the proposed technique selected the best sub-features that achieved a higher classification accuracy than the sub-features selected by a single-level relief or PSO selector.

The selected features by Relief, PSO and Cascaded Bi-level feature selectors used for training and testing of the four models are presented in Table 8.

From Table 8, for the Mathematics dataset Relief selector selected 20 feature sets from the 32 original feature sets, PSO selected 16 features and cascaded bi-level selector selected 11 features from the original feature sets. For the Portuguese dataset Relief selector selected 20 feature sets from the 32 original feature sets, PSO selected 14 features and cascaded bi-level selector selected 8 features

from the original feature sets. From the selected features in Table 5 it can be seen that the G1 and G2 features were selected by all the feature selectors. This shows that first period grade (G1) and the second period grade (G2) are relevant for the final grade prediction.

Table 8. Selected feature sets by Relief, PSO and Cascaded bi-level feature selectors for binary-level grading

	Selected Feature sets	
	MATHEMATICS	**PORTUGUESE**
Relief	G2, G1, Sex, Paid, Failures, Activities, Romantic, Famsup, Stidytime, Higher, Mjob, Pstatus, Dalc, Medu, Guardian, Goout, Walc, Absences, Age, School	School, G2, G1, Activities, Sex, Address, Famsup, Failures, Nursery, Reason, Romantic, Higher, Medu, Famrel, Schoolsup, Fedu, Internet, Goout, Studytime, Health
PSO	School, Age , Famsize, Medu, Fjob, Guardian, Failures, Famsup, Paid, Activities, Nursery, Internet, Romantic, Freetime, G1, G2	Age, Address, Famsize, Fjob, Reason, Traveltime, Studytime, Failures, Famsup, Paid, Freetime, Goout, G1, G2
Cascaded Bi-Level	G2, G1, Sex, Activities, Famsup, Studytime, Mjob, Medu, Guardian, Goout, Walc	G2, G1,Nursery, Reason, Romantic, Higher, Schoolsup, Goout

Table 9 presents a comparison of the performance of the proposed technique with related work that used the student performance dataset from UCI repository with respect to binary classification. The results obtained showed

that the proposed technique achieved a higher student prediction accuracy than related work.

Table 9. Comparison of Binary Classification Performance with Related Work

	Mathematics	Portuguese
Techniques	**Highest Obtained Accuracy (%)**	**Highest Obtained Accuracy (%)**
Ünal [14]	93.67	93.22
Shah [35]	93.80	
Cascaded Bi-level	**94.94**	**96.15**

4.2 Five-Level Grading Classification

The five-level grading classification deals with classification using the five classes which are excellent (5), good (4), satisfactory (3), sufficient (2) and fail (1). The original label of 0-20 labels or grades were categorized into the aforementioned five classes. Using the five-level grading the four classifiers (ECOC, Ensemble, KNN and Decision Tree) were trained and tested using the original features (no feature selection done), sub-features using relief feature selector, sub-features using PSO feature selector and sub-features using a cascade bi-level feature selector. The five-level grading classification result is shown in Table 6.

From Table 10 it can be seen that ensemble classifiers performed best for both Mathematics and Portuguese dataset with an accuracies of 72.68% and 80.05% respectively. DT also performed least for both Mathematics and Portuguese dataset with accuracies of 64.56%, and 76.92% respectively. Table 11 presents the accuracy, precision, recall and f-score of all the four classifiers when trained with the Relief selected sub-features.

To properly evaluate the performance of ECOC, Ensemble, DT and KNN classifiers when trained with Relief selected feature subsets for both Mathematics and Portuguese data set for the five-level grading version, their precision, recall, f-score and accuracy are presented in Table 11. The ensemble classifier performed best with an accuracy of 79.75% and f-score of 91.80% for Mathematics dataset. While ECOC performed best with an accuracy of 93.08% and f-score of 82.35% for Portuguese dataset.

Table 12 is classification results of ECOC, Ensemble, KNN and DT when trained with PSO selected feature sets. In Table 12 Ensemble classifier obtained the best performance for both Mathematics and Portuguese data

Table 10. Five-level classification results before feature selection

Before Feature Selection Classification Results							
	Mathematics				Portuguese		
Classifiers	**Accuracy (%)**	**F-Score (%)**	**Precision (%)**	**Recall (%)**	**Accuracy (%)**	**F-Score (%)**	**Precision (%)**	**Recall (%)**
ECOC	72.42	77.73	85.00	71.67	72.31	80.00	72.73	88.89
Ensemble	72.68	78.33	86.01	72.98	74.62	80.05	70.73	92.12
KNN	69.62	73.33	73.33	73.33	70.77	76.92	68.18	88.24
DT	64.56	68.45	68.45	68.45	66.15	78.82	78.82	78.82

Table 11. Five-level Classification for Relief Selected Features

Relief Selected Features Classification Results							
	Mathematics				Portuguese		
Classifiers	**Accuracy (%)**	**F-Score (%)**	**Precision (%)**	**Recall (%)**	**Accuracy (%)**	**F-Score (%)**	**Precision (%)**	**Recall (%)**
ECOC	75.95	88.52	84.38	93.10	93.08	82.35	80.77	84.00
Ensemble	79.75	91.80	87.50	95.25	93.08	81.63	76.92	86.96
KNN	75.95	87.50	87.50	87.50	91.54	77.55	73.08	82.61
DT	70.89	85.25	81.25	89.66	92.31	79.17	82.61	86.36

Table 12. Five-level Classification for PSO Selected Features

PSO Selected Features Classification Results							
	Mathematics				Portuguese		
Classifiers	**Accuracy (%)**	**F-Score (%)**	**Precision (%)**	**Recall (%)**	**Accuracy (%)**	**F-Score (%)**	**Precision (%)**	**Recall (%)**
ECOC	75.95	78.26	75.00	81.82	77.69	77.78	77.78	77.78
Ensemble	78.48	80.85	79.17	82.26	78.64	78.28	69.23	90.00
KNN	74.68	80.00	75.00	85.71	76.92	76.92	76.92	76.92
DT	72.15	78.26	75.00	81.82	71.77	62.52	76.92	52.63

sets with an accuracy of 78.26% and an f-score of 80.85% for Mathematics data set and an accuracy of 78.64% and an f-score of 78.28% for Portuguese data set. For both Mathematics and Portuguese data set DT performed least with an accuracy of 72.15% and f-score of 78.26% for Mathematics data set and accuracy of 71.77% and f-score of 62.52% for Portuguese data set.

In Table 13 the Ensemble classifier produced the best performance for both the Mathematics and Portuguese data sets. Ensemble classifier got an accuracy of 84.81%, f-score of 92.31%, precision of 93.75% and recall of 90.91% for Mathematics dataset. For the Portuguese data set the Ensemble classifier obtained an accuracy of 83.85%, f-score of 87.50%, precision of 77.78% and recall of 100%. Table 14 is a comparison of the performance based on accuracy of the Relief, PSO and Cascaded bi-level feature selection techniques.

In Table 14 the highest classification accuracy which was obtained by Ensemble classifier using the Relief selected features for the Mathematics data set is 79.75%. The PSO selected sub-features obtained a classification accuracy of up to 78.48% from Ensemble classifier for the Mathematics data set. The proposed cascaded bi-level obtained the highest accuracy of 84.81% when compared with Relief and PSO performance for the Mathematics data set. For the Portuguese data set the highest classification accuracy obtained for classification using the Relief selected features is 76.92% by Ensemble classifier. The PSO selected sub-features obtained a classification accuracy of up to 78.64% for the Portuguese data set using the Ensemble classifier. The proposed cascaded bi-level obtained highest accuracy of 83.85% when compared with Relief and PSO performance for the Portuguese data set. Training with the original complete 32 feature sets obtained the least accuracy as compared with training with the selected Relief, PSO and Cascaded bi-level feature sets. In conclusion the proposed technique selected the best sub-features that achieved a higher classification accuracy than the sub-features selected by a single-level relief or PSO selector.

From Table 15, for the Mathematics dataset Relief feature selector selected 20 feature sets from the 32 original feature sets, PSO selected 16 features and cascaded bi-level selector selected 10 features from the original feature sets. For the Portuguese dataset Relief selector selected 20 feature sets from the 32 original feature sets, PSO selected 13 features and cascaded bi-level selector selected 6 features from the original feature sets. From the selected features in Table 8 it can be seen that the G1 and G2 features were selected by all the feature selectors. This shows that first period grade (G1) and the second period grade (G2) is relevant for the final grade prediction for the five-level grading as it is important in the binary-level grading classification task.

Table 13. Five-level Classification for Cascaded Bi-level Selected Features

| | Cascaded Bi-level Selected Features Classification Results | | | | | | | |
| | Mathematics | | | | Portuguese | | | |
Classifiers	Accuracy (%)	F-Score (%)	Precision (%)	Recall (%)	Accuracy (%)	F-Score (%)	Precision (%)	Recall (%)
ECOC	83.54	90.00	84.38	96.43	83.08	88.24	83.33	93.75
Ensemble	84.81	92.31	93.75	90.91	83.85	87.50	77.78	100
KNN	81.01	88.14	81.25	96.30	77.38	74.29	72.22	76.47
DT	73.42	81.97	78.13	86.21	72.67	76.19	88.89	66.77

Table 14. Comparison of Feature Selection Techniques for Five-level Classification Task

| | Accuracy (%) | | | | | | | |
| | Mathematics | | | | Portuguese | | | |
Feature Selection	ECOC	Ensemble	KNN	DT	ECOC	Ensemble	KNN	DT
Before Feature Selection	72.42	72.68	69.62	64.56	72.31	74.62	70.77	66.15
Relief	75.95	79.75	75.95	70.89	76.15	76.92	74.62	72.31
PSO	75.95	78.48	74.68	72.15	77.69	78.64	76.92	71.77
Cascaded Bi-level	83.54	84.81	81.01	73.42	83.08	83.85	77.38	72.67

Table 15. Selected feature sets by Relief, PSO and Cascaded bi-level feature selectors for Five-level grading

	Selected Feature sets	
	MATHEMATICS	**PORTUGUESE**
Relief	G2, G1, Sex, Medu, Walc, Studytime, Address, Paid, Schoolsup, Mjob, Failures, Higher, Pstatus, Dalc, school, Freetime, Age, Famsup, Internet, Absences	G2, G1, School, Activities, sex, Studytime, Higher, Medu, Failures, Schoolsup, Nursery, Health, Famsup, Goout, Pstatus, Address, Fedu, Internet, Reason, Walc
PSO	Sex, Age, Famsize, Medu, Failures, Schoolsup, Famsup, Paid, Activities, Nursery, Internet, Romantic, Famrel, Freetime, G1, G2	Sex, Medu, Failures, Schoolsup, Paid, Activities, Internet, Famrel, Freetime, Goout, Health, G2, G1
Cascaded Bi-level	G2, G1, Walc, Studytime, Address, Paid, Schoolsup, Failures, Dalc, Internet	G2, G1, sex, Famsup, Pstatus, Address

Table 16 presents a comparison of the performance of the proposed technique with related works that used the Student performance dataset from UCI repository with respect to five-level grading classification. The results obtained showed that the proposed technique achieved a higher student prediction accuracy than related works based on Portuguese and Mathematics data set.

Table 16. Comparison of Five-Level Grading Performance with Related Work

Techniques	Mathematics	Portuguese
	Highest Obtained Accuracy (%)	**Highest Obtained Accuracy (%)**
Salal [12]		76.73
Ünal [14]	79.49	77.20
Proposed Technique	**84.81**	**83.85**

5. Conclusions - Future Works

This study developed a cascade bi-level feature selection technique for predicting students' academic performance. The Cascade bi-level feature selection technique achieved using Relief filter-based algorithm and Particle Swarm Optimization (PSO) algorithm. First the relief algorithm was used to select features based on their relevance to the target class. This selected features were fed as input to the PSO. The PSO then optimally selects the subset of the selected features based on the particle fitness. The Relief, PSO, and the Cascade bi-level selected features were analyzed using Error-Correcting Output Code (ECOC), ensemble, Decision Tree and K-Nearest Neighbour (KNN) machine learning models. The cascaded bi-level feature selection technique was evaluated against single-level feature selection techniques and against related works. The accuracy performance metric was used to perform this assessment. The proposed cascaded bi-level feature selection technique obtained an accuracy of 94.94% for Mathematics data set and 96.15% for Portuguese data set using the binary-level grading version

of the data set. The cascaded bi-level feature selection technique also obtained an accuracy 84.81% for Mathematics data set and 83.85% for Portuguese data set using the five-level grading version of the data set. The results indicate the effectiveness of the cascaded bi-level feature selection technique in achieving an improved student performance prediction as it selects the best sub-features.

This study utilized Relief a filter-based technique and Particle swarm optimization a wrapper technique for feature selection. For future work other filter and wrapper-based feature selection techniques can be utilized, which can provide an insight on which filter and/or wrapper-based selection techniques produces better results when combined. In this study, the bi-level selection approach was considered. It is recommended that further research should explore multiple-level techniques for feature selection.

References

[1] J. M. Adán-Coello and C. M. Tobar, 'Using Collaborative Filtering Algorithms for Predicting Student Performance', in *Electronic Government and the Information Systems Perspective*, vol. 9831, A. Kő and E. Francesconi, Eds. Cham: Springer International Publishing, 2016, pp. 206-218.
DOI: 10.1007/978-3-319-44159-7_15.

[2] E. Jembere, R. Rawatlal, and A. W. Pillay, 'Matrix Factorisation for Predicting Student Performance', in *2017 7th World Engineering Education Forum (WEEF)*, Kuala Lumpur, Nov. 2017, pp. 513-518.
DOI: 10.1109/WEEF.2017.8467150.

[3] K. David Kolo, S. A. Adepoju, and J. Kolo Alhassan, 'A Decision Tree Approach for Predicting Students Academic Performance', *Int. J. Educ. Manag. Eng.*, vol. 5, no. 5, pp. 12-19, Oct. 2015.
DOI: 10.5815/ijeme.2015.05.02.

[4] S. Hussain, N. Abdulaziz Dahan, F. M. Ba-Alwi, and N. Ribata, 'Educational Data Mining and Analysis

of Students' Academic Performance Using WEKA', *Indones. J. Electr. Eng. Comput. Sci.*, vol. 9, no. 2, p. 447, Feb. 2018.
DOI: 10.11591/ijeecs.v9.i2.pp447-459.

[5] M. Imran, S. Latif, D. Mehmood, and M. S. Shah, 'Student Academic Performance Prediction using Supervised Learning Techniques', *Int. J. Emerg. Technol. Learn. IJET*, vol. 14, no. 14, p. 92, Jul. 2019.
DOI: 10.3991/ijet.v14i14.10310.

[6] M. A. Amoo, O. B. Alaba, and O. L. Usman, 'Predictive modelling and analysis of academic performance of secondary school students: Artificial Neural Network approach', *Int. J. Sci. Technol. Educ. Res.*, vol. 9, no. 1, pp. 1-8, May 2018.
DOI: 10.5897/IJSTER2017.0415.

[7] Z. M. Hira and D. F. Gillies, 'A Review of Feature Selection and Feature Extraction Methods Applied on Microarray Data', *Adv. Bioinforma.*, vol. 2015, pp. 1-13, Jun. 2015.
DOI: 10.1155/2015/198363.

[8] A. Daud, N. R. Aljohani, R. A. Abbasi, M. D. Lytras, F. Abbas, and J. S. Alowibdi, 'Predicting Student Performance using Advanced Learning Analytics', in *Proceedings of the 26th International Conference on World Wide Web Companion - WWW '17 Companion*, Perth, Australia, 2017, pp. 415-421.
DOI: 10.1145/3041021.3054164.

[9] B. K. Francis and S. S. Babu, 'Predicting Academic Performance of Students Using a Hybrid Data Mining Approach', *J. Med. Syst.*, vol. 43, no. 6, p. 162, Jun. 2019.
DOI: 10.1007/s10916-019-1295-4.

[10] E. T. Lau, L. Sun, and Q. Yang, 'Modelling, prediction and classification of student academic performance using artificial neural networks', *SN Appl. Sci.*, vol. 1, no. 9, p. 982, Sep. 2019.
DOI: 10.1007/s42452-019-0884-7.

[11] A. M. Olalekan, O. S. Egwuche, and S. O. Olatunji, 'Performance Evaluation Of Machine Learning Techniques For Prediction Of Graduating Students In Tertiary Institution', in *2020 International Conference in Mathematics, Computer Engineering and Computer Science (ICMCECS)*, Ayobo, Ipaja, Lagos, Nigeria, Mar. 2020, pp. 1-7.
DOI: 10.1109/ICMCECS47690.2020.240888.

[12] Y. K. Salal, S. M. Abdullaev, and M. Kumar, 'Educational Data Mining: Student Performance Prediction in Academic', vol. 8, no. 4, p. 6, 2019.

[13] A. Magbag and R. R. Jr, 'Prediction Of College Academic Performance Of Senior High School Graduates Using Classification Techniques', vol. 9, no. 04,

p. 6, 2020.

[14] F. Ünal, 'Data Mining for Student Performance Prediction in Education', *IntechOpen*, p. 12, 2020.
DOI: http://dx.doi.org/10.5772/intechopen.91449.

[15] P. Cortez and A. Silva, 'Using data mining to Predict Secondary School Student Performance', p. 9, 2008.

[16] C. Seger, 'An investigation of categorical variable encoding techniques in machine learning: binary versus one-hot and feature hashing', Bachelor Degree, KTH ROYAL INSTITUTE OF TECHNOLOGY SCHOOL OF ELECTRICAL ENGINEERING AND COMPUTER SCIENCE, Sweden, 2018.

[17] J. Wang, S. Zhou, Y. Yi, and J. Kong, 'An Improved Feature Selection Based on Effective Range for Classification', *Sci. World J.*, vol. 2014, pp. 1-8, 2014.
DOI: 10.1155/2014/972125.

[18] B. Kumari and T. Swarnkar, 'Filter versus Wrapper Feature Subset Selection in Large Dimensionality Micro array: A Review', vol. 2, p. 6, 2011.

[19] R. P. L. Durgabai and Y. Ravi Bhushan, 'Feature Selection using ReliefF Algorithm', *IJARCCE*, pp. 8215-8218, Oct. 2014.
DOI: 10.17148/IJARCCE.2014.31031.

[20] R. J. Urbanowicz, R. S. Olson, P. Schmitt, M. Meeker, and J. H. Moore, 'Benchmarking Relief-Based Feature Selection Methods for Bioinformatics Data Mining', *ArXiv171108477 Cs*, Apr. 2018, Accessed: Jul. 13, 2021. [Online]. Available: http://arxiv.org/abs/1711.08477.

[21] S. Talukder, 'Mathematical Modelling and Applications of Particle Swarm Optimization', Master's Thesis, Blekinge Institute of Technology, 2011.

[22] S. Sengupta, S. Basak, and R. A. P. Ii, 'Particle Swarm Optimization: A survey of historical and recent developments with hybridization perspectives', p. 34, 2019.

[23] B. Sahu and D. Mishra, 'A Novel Feature Selection Algorithm using Particle Swarm Optimization for Cancer Microarray Data', *Procedia Eng.*, vol. 38, pp. 27-31, 2012.
DOI: 10.1016/j.proeng.2012.06.005.

[24] G. Armano, C. Chira, and N. Hatami, 'Error-Correcting Output Codes for Multi-Label Text Categorization', p. 12, 2013.

[25] S. Escalera, O. Pujol, P. Radeva, and P. Ivanova, 'Error-Correcting Ouput Codes Library', *J. Mach. Learn. Res.*, vol. 11, p. 4, 2010.

[26] A. S. Olaniyi, S. Y. Kayode, H. M. Abiola, S.-I. T. Tosin, and A. N. Babatunde, 'STUDENT'S PERFORMANCE ANALYSIS USING DECISION TREE ALGORITHMS', *Int. J. Comput. Eng. Res.*,

vol. 08, no. 9, p. 8, Sep. 2018.

[27] I. Bukovsky, W. Kinsner, and N. Homma, 'Learning Entropy as a Learning-Based Information Concept', *Entropy*, vol. 21, no. 166, pp. 1-14, 2019. DOI: 10.3390/e21020166.

[28] Z. Zhang, 'Introduction to machine learning: k-nearest neighbors', *Ann. Transl. Med.*, vol. 4, no. 11, pp. 218-218, Jun. 2016. DOI: 10.21037/atm.2016.03.37.

[29] S. P. Arade and J. K. Patil, 'COMPARATIVE STUDY OF DIABETIC RETINOPATHY USING K-NN AND BAYESIAN CLASSIFIER', *Int. J. Innov. Eng. Res. Technol.*, vol. 4, no. 5, pp. 55-61, 2017.

[30] A. Kataria and M. D. Singh, 'A Review of Data Classification Using K-Nearest Neighbour Algorithm', *Int. J. Emerg. Technol. Adv. Eng.*, vol. 3, no. 6, pp. 354-360, 2013.

[31] X. Gu, L. Akoglu, and A. Rinaldo, 'Statistical Analysis of Nearest Neighbor Methods for Anomaly Detection', in *33rd Conference on Neural Information Processing Systems*, canada, 2019, p. 11.

[32] E. A. Amrieh, T. Hamtini, and I. Aljarah, 'Mining Educational Data to Predict Student's academic Performance using Ensemble Methods', *Int. J. Database Theory Appl.*, vol. 9, no. 8, pp. 119-136, Aug. 2016. DOI: 10.14257/ijdta.2016.9.8.13.

[33] O. W. Adejo and T. Connolly, 'Predicting student academic performance using multi-model heterogeneous ensemble approach', *J. Appl. Res. High. Educ.*, vol. 10, no. 1, pp. 61-75, Feb. 2018. DOI: 10.1108/JARHE-09-2017-0113.

[34] A. Almasri, E. Celebi, and R. S. Alkhawaldeh, 'EMT: Ensemble Meta-Based Tree Model for Predicting Student Performance', *Sci. Program.*, vol. 2019, pp. 1-13, Feb. 2019. DOI: 10.1155/2019/3610248.

[35] M. B. Shah, M. Kaistha, and Y. Gupta, 'Student Performance Assessment and Prediction System using Machine Learning', in *2019 4th International Conference on Information Systems and Computer Networks (ISCON)*, Mathura, India, Nov. 2019, pp. 386-390. DOI: 10.1109/ISCON47742.2019.9036250.

ARTICLE

Web Application Authentication Using Visual Cryptography and Cued Clicked Point Recall-based Graphical Password

Mary Ogbuka Kenneth[1*]   Stephen Michael Olujuwon[2]

1. Department of Computer Science, Federal University of Technology, Minna, Nigeria
2. Department of Cyber Security Science, Federal University of Technology, Minna, Nigeria

ABSTRACT

Alphanumerical usernames and passwords are the most used computer authentication technique. This approach has been found to have a number of disadvantages. Users, for example, frequently choose passwords that are simple to guess. On the other side, if a password is difficult to guess, it is also difficult to remember. Graphical passwords have been proposed in the literature as a potential alternative to alphanumerical passwords, based on the fact that people remember pictures better than text. Existing graphical passwords, on the other hand, are vulnerable to a shoulder surfing assault. To address this shoulder surfing vulnerability, this study proposes an authentication system for web-applications based on visual cryptography and cued click point recall-based graphical password. The efficiency of the proposed system was validated using unit, system and usability testing measures. The results of the system and unit testing showed that the proposed system accomplished its objectives and requirements. The results of the usability test showed that the proposed system is easy to use, friendly and highly secured.

1. Introduction

Passwords, which are the most important aspect of the authentication process, are crucial to information and computer security. Authentication is the act of a system verifying a user's identity. It's a method of determining if a specific person or device should have access to a system, an application, or just an object operating on a device [1]. Authentication refers to the act of only showing the valuables to their rightful owner. Authentication is also the first line of defense in safeguarding any resource. A password is a type of secret authentication data utilized to control resource access. Those who are not given access are kept in the dark about the password, while those who

seek to get access are tested to see if they know it and then granted or denied access appropriately. Passwords are required for a variety of tasks by a normal computer user, including login into accounts, getting email from servers, databases, networks, accessing data, and web sites, and even reading the morning newspaper online [2]. Nowadays, a variety of user authentication mechanisms are accessible. The most prevalent way of computer authentication is to utilize an alphanumeric username and password, which has a number of disadvantages. Since the system's developer sees alphanumeric passwords as a string of characters, they are simple to implement [3]. A properly safe password, on the other hand, should be both random and easy to remember. Randomness prevents an attacker

Corresponding Author:
Mary Ogbuka Kenneth,
Department of Computer Science, Federal University of Technology, Minna, Nigeria;
Email: kenneth.pg918157@st.futminna.edu.ng

from guessing the password, while a memorable password makes it easier for the owner to get access. However, this is difficult to achieve using alphanumeric passwords, because a random string of characters that cannot be quickly guessed is more difficult for the owner to remember. A basic password, on the other hand, will be easily remembered by the owner but will be easy to determine by an attacker, rendering it usable but vulnerable [4]. To alleviate the problem with alphanumeric authentication, a large variety of graphical password schemes have been created and tested [5]. One explanation for the surge in popularity of graphical passwords is because visuals, as opposed to strings of characters, are thought to be more remembered. Using graphics or drawings as passwords is referred to as graphical passwords. Graphical passwords should be easier to remember in theory because humans recall pictures better than words [2]. In addition, because the search space is nearly endless, they should be more resistant to brute-force attacks. In general, there are two types of graphical password techniques: recognition-based and recall-based graphical passwords techniques. A user gets authenticated using recognition-based techniques by asking him or her to identify one or more photos at the registration phase. During Login, a user is asked to reproduce anything that he or she developed or selected earlier during the registration step in recall-based procedures [6].

The vulnerability of traditional password schemes to shoulder surfing and key-logging attacks is one of their drawbacks. Shoulder surfing happens when someone looks over your shoulder as you enter sensitive information into an electronic device, such as your ATM PIN, password, or credit card number [7]. Key-logging is a type of malicious software that records keystrokes on a keyboard without the user's awareness [8]. Key-loggers are difficult to detect because they operate in stealth mode or masquerade as genuine program on the computer [9]. There are numerous methods for combating the threat of key-loggers, but none of them is adequate on its own. To effectively solve the problem, a mix of techniques is required [10]. Using a combination of visual cryptography and graphical password, this study seeks to overcome the problem of shoulder-surfing and key-logging attacks. The followings are the study's main contributions:

(1) Development of a secure cryptographic system.
(2) Development of a secure graphical password authentication system.

The following is how the rest of the paper is structured: A summary of related researches on graphical authentication is included in section two. The techniques used to accomplish the goal of authentication are presented in section three. In section four results from the experimentation are presented and discussed. The study's conclusion is presented in section five and lastly future works are presented in section six.

2. Related Works

The limits of graphical and alphanumeric passwords were identified by Chuen [11]. One of the drawbacks of using a graphical password technique is the possibility of shoulder surfing. A graphical password could be physically witnessed, especially in public locations, and if the attacker has a clearer vision of the password being entered several times, they could easily decipher the password, which is a serious weakness. Another disadvantage of a graphical password technique is that it is vulnerable to guessing. If the user only registered a brief and predictable password, the odds of it being guessable would rise, just like with an alphanumeric password. To conquer these potential drawbacks, a shoulder surfing-resistant method could be enacted, such as including multiple mouse cursors when users log in to their accounts, which would make it difficult for the attacker to determine which mouse cursors are valid and which click points the user has clicked. Next, a prerequisite of at least 10 click points to make the graphical password harder, similar to an alphanumeric password, could be enforced to the system to ensure that the user does not simply enter a sloppy password, reducing the chances of an attacker guessing the user's password significantly.

Vaddeti [12] suggested a graphical password authentication scheme based on the best existing features like hash index, distorted images, and loci metrics, as well as visual cryptographic techniques and additional naive features, to defend against well-known attacks like brute-force, educated guessing, sniffing, hidden camera, shoulder surfing, and phishing. The paper's flaw is that no assessment metric was utilised to assess the system's performance.

Shnain and Shaheed [13] employed pictorial passwords to improve E-commerce authentication problems. A modified Inkblot authentication method was presented in this paper. Images are used as a trigger for text password entry in the Inkblot authentication method. Users are given the option of selecting a series of inkblots and typing in the first and last letter of the word/phrase that best describes the inkblot during password creation. The user's password is made up of these pairs of letters. The inkblot is a useful tool for users to create their login. The problem with this inkblot authentication method is that users are only given a limited number of password options.

Ahsan and Li [14] presented a graphical password authentication employing an image sequence. In this manner, the user uploads photographs from his or her own

directory for password selection, and the images supplied by one user are not visible to the other. The planned system is divided into four phases. The legitimate email address stage is the first step. The user will submit a genuine email address during registration, which will be used throughout the login phase. The system will redirect the visitor to the next page after inputting a valid email address, which will provide photographs for selection. The second stage is the picture selection phase, in which a user can choose between a maximum of six and a minimum of four photographs to finish the registration process. A user will be asked to pick the amount of photographs that were uploaded during the registration step after logging in. Users upload their desired photographs based on the prior number of images picked in the third phase. In the last phase, the picked photos are stored in order. When logging in, the user selects uploaded photographs in the same order as they were picked during the registration step. The user will not be able to login if the sequence of selected photos is incorrect. The suggested technique is vulnerable to shoulder surfing, because an assault can readily capture the image sequence during registration or login.

Dana [15] developed on a visual cryptography system that allows visual information to be encoded in such a way that it can be decrypted solely by sight. The encoding of the original image is split into two images in this method of cryptography by changing every pixel into a pattern that looks like grey or noise. The User ID was extracted from the server share using an optical character recognition method. As a result, a user's identity is verified by matching the retrieved and preserved IDs. Using optical character recognition raises the computational complexity of the procedures, which is a disadvantage.

Togookhuu [16] suggested a three-layer verification recall graphical password technique. The suggested recall-based authentication technique was an upgrade to the Pass-Go scheme, which included secret questions, answers, and backdrop imagery. The suggested system, dubbed CRS, is made up of three pieces that work together to ensure password security. The initial portion of the verification process is concerned with the secret question and the text-based answer. The second section is about selecting a picture based on recognition, and the third section is about constructing a password using a drawing that is easy to remember. The disadvantage of this method is that it is easy for people to forget their stroke order while using drawing to create a password.

3. Methodology

The proposed technique implements a two level graphical password schemes to provide more security to avoid should surfing attack and key-logging attack. The first level of authentication is the visual cryptography authentication and the second level of authentication is the cued click point recall-based authentication. The two level graphical passwords are embedded in two phases namely: Registration phase and the login phase. These phases and level are discussed in detail below. The proposed system was implemented using PHP, HTML, CSS, MYSQL, JavaScript and Python.

3.1 System Design

3.1.1 Architectural Design

Architectural design is all about understanding how a system should be organized and constructing the overall structure of that system. The architectural design is the first step of the software development process. It is the crucial link between design and requirements engineering since it defines the system's primary structural components and their relationships. Figure 1 depicts the suggested system design.
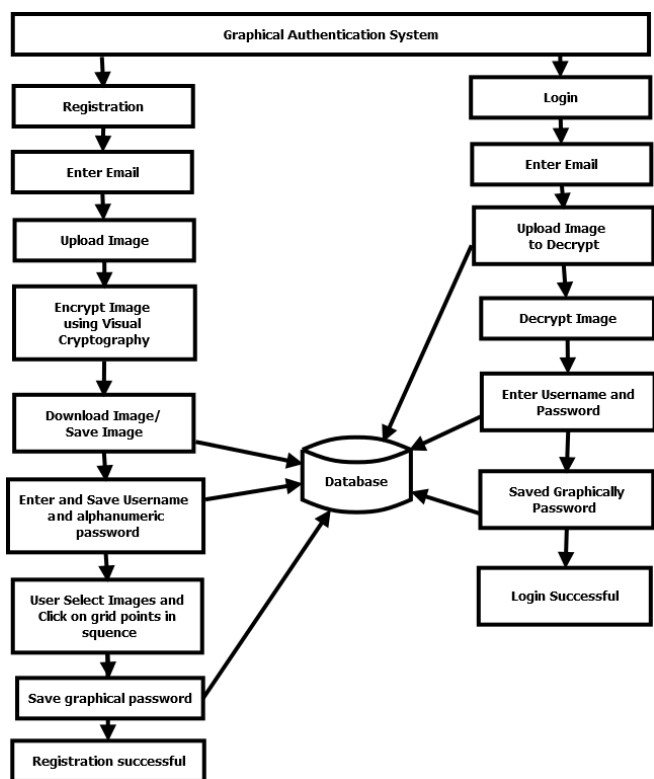

Figure 1. Proposed System Architecture

In Figure 1, the architectural design involves the process function, system database, and the external entities that will interact with the system. The authentication system in Figure 1 consists of two phases: registration and login phase. The registration phase involves the image

encryption using visual cryptography, alphanumeric password registration and the graphical password registration. The login phase involves shared image authentication, password verification and graphical password validation.

3.1.2 Flowchart of the Proposed System

A flowchart is a graphical depiction of a series of steps. It is commonly used to show the flow of algorithms, workflows, or processes in a sequential order [17]. Figure 2 depicts the suggested system flowchart.

The flowchart in Figure 2 shows the flow of events from the beginning to the end of the registration and login phase. In each stage of the login activity a validation process takes place. For example the shared image is validated, the username and password is validated and also the graphical password is validated. The registration or sign up activity is straightforward as it deals with just receiv-

ing the user's choice of images, username, and password as inputs for verification purpose.

3.2 Proposed Techniques

The proposed system consists of mainly of two techniques in sequential order: visual cryptography and graphical password. Each of these techniques is explained in detail in this section.

3.2.1 Visual Cryptography (VC) Authentication

The graphical password authentication scheme's initial stage is Visual Cryptography (VC). VC is a sophisticated approach that blends the concepts of cryptography's perfect cyphers and secret sharing with raster graphics [18]. Visual cryptography is a cryptography method that allows visual information (pictures and text) to be encoded and decoded in such a way that the decoded data appear as
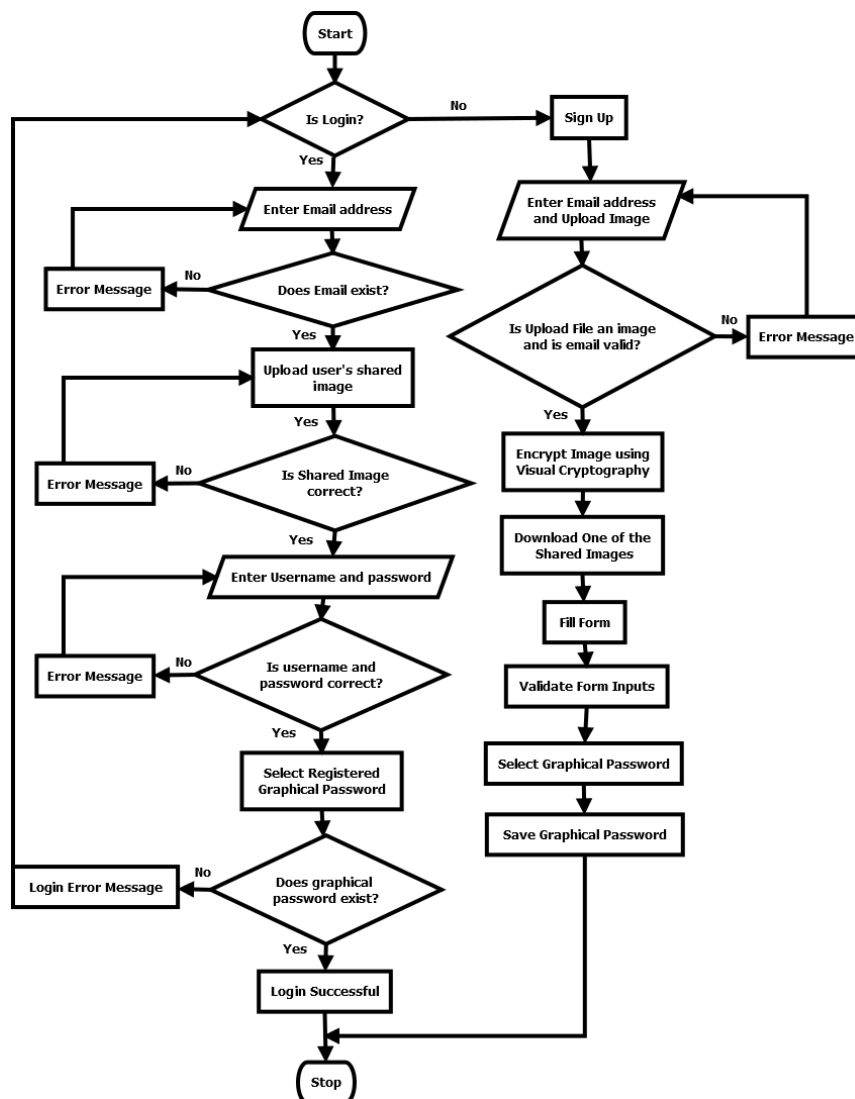

Figure 2. Flowchart for the Proposed Authentication System

a visual image. A binary image can be split into shares, which can then be stacked to resemble the original image. A secret sharing technique allows a secret to be distributed among n parties, with only predefined approved sets being able to reconstruct it [19]. In terms of VC, the secret can be visually reconstructed by superimposing shares. VC enables the transfer of visual data, and many facets of this field are discussed, from its inception to current approaches that are being used and actively researched today. This assessment looks at the progress of VC, as well as contemporary trends and applications [18]. It is quite desirable to be able to conceal information such as personal information. The data are completely unrecognizable when it is concealed within distinct images (known as shares). The data are entirely incomprehensible, despite the fact that the shares are separate. Each image contains distinct pieces of data, and when they are combined, the secret may be easily discovered. In order to access the decrypted information, they each depend on one another. Anyone should be unable to read the information stored within any of the shares. When the shares are brought together and stacked on top of one another, decoding is possible. The information becomes instantaneously available at this point. The information can be decrypted with no computational resources at all [20].
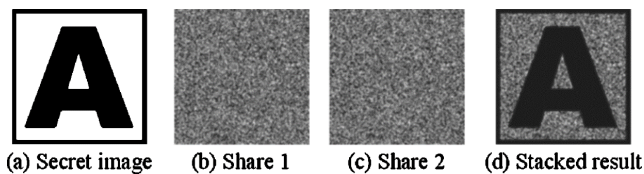

(a) Secret image (b) Share 1 (c) Share 2 (d) Stacked result

Figure 3. Results of a Visual Cryptography Scheme

Figure 3 shows the implementation and results of basic visual cryptography. It displays the secret image, the two shares that are generated and the recovery of the secret after superimposing share one and share two.

3.2.2 Cued Click Point Recall-Based Authentication

In this strategy, the system provides certain tips that assist users in accurately reproducing their passwords. Hot spots (regions) inside an image will be used to provide these hints [1]. To register as a password, the user must select one of these regions, and to log into the system, they must select the same region in the same order. Cued Click Points (CCP), a recall-based approach, was employed for user authentication in this study. A potential replacement to Pass-Points is Cued Click Points (CCP) [4]. In CCP, users click one point on each image rather than several points on a single image. It has cued-recall and visual cues that immediately notify valid users if they make a mistake when entering their most recent click-point. It also makes hotspot analysis-based attacks more difficult [21].

A wrong click progresses down the wrong path, with verification failure being explicitly indicated only after the final click. Users can only choose their images to the extent that the next image is dictated by their click-point. If they don't like the images that come up, they can make a new password with different click-points to achieve other results. CCP works in the same way as Pass-Points when it comes to implementation. A discretization approach is utilized to identify a click-tolerance point's square and associated grid during password formation. This grid is obtained and used to determine if each click-point on a subsequent login attempt falls within the tolerance of the originating point [21]. Being cued to recall one point on each of the three photos appears to be easier than recalling an ordered sequence of three points on one image, which is a usability benefit of CCP. Figures 4 and 5 illustrate
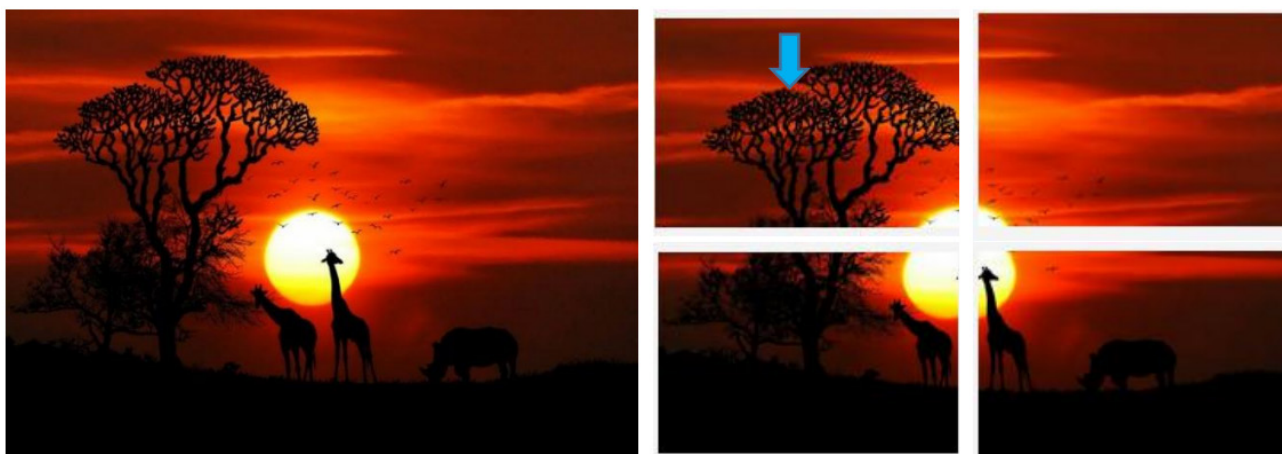

Figure 4. first selected image in the Cue Clicked Point process

Figure 5. Second selected image in the Cue Clicked Point process

an example of a 2 × 2 grid of two selected photos for the CCP procedure.

In Figure 4, a user selects the first image at the left, the selected image is then divided into four images shown in the right. A user now clicks to select one from this sub-images. After clicking one of the sub-images another image is loaded as shown in Figure 5 for another selection. The second selected image is also divided into four sub-images, in which the user also clicks and selects from the sub-images. After the second sub-image is selected another third image is loaded and the process continues.

Registration phase

The registration phase consists of three main processes: visual cryptography, input data and CCP implementation. The registration phase is presented in Figure 6 and the steps involved in the registration phase are discussed below.
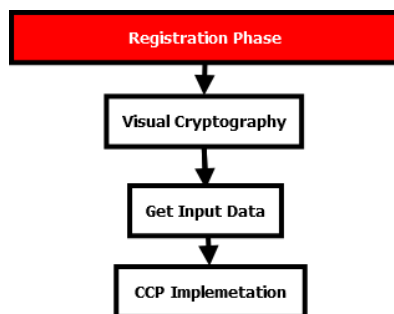

Figure 6. Registration Phase

- **Step 1: Visual cryptography**

In this phase the user is asked to upload an image of their choice. This uploaded image is then encrypted and converted into two shared images using visual cryptography technique. The user is then prompted to download and save one among these two images. This generated images are stored in the database for further use.

- **Step 2: Get Data**

The get data phase obtains the details of users such as user-id, email-id, password, full name and phone number.

- **Step 3: CCP implementation**

A 2 × 2-image grid is now displayed to the user from which the user clicks on one point of the image. After which, the user is to select another image and click on the generated 2 × 2-image grid.

Login and authentication phase

The login and authentication phase is depicted in Figure 7. The steps involve in also in the login phase is discussed below.
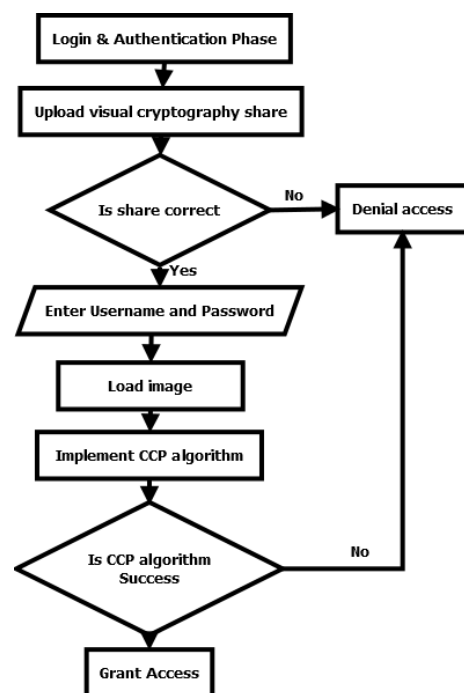

Figure 7. Login and Authentication Phase

- **Step 1: Share Submission (Visual Cryptography)**

During the login phase, the user shared image must be submitted which is compared with the shares stored in the database. If shared images match then the user is allowed to move to the next step.

- **Step 2: Username and Password Authentication**

In this step the user is asked to supply their registered username and password. If a wrong username and password is supplied the access is denied. However if the username and password is correct the user is given access to the next authentication process.

- **Step 3: Graphical password (Cued Clicked point)**

After authenticating the username and password, five images are displayed. The user is prompted to select one of the displayed images. On click of an image a 2 x 2 grid containing parts of the selected image is displayed user is expected to click on the grid in image for successful authentication. If the first attempt fails, the user is asked to login from the beginning.

Another significant point to be noticed in the proposed scheme is no image is highlighted when user clicks the images during login phase in order to prevent shoulder surfing and hidden camera based attacks. The Proposed system was implemented using PHP, HTML, CSS, and Python.

3.3 Evaluation Metrics

Software evaluation refers to the examination of the program itself to see if it works or has any errors or bugs. Evaluation of the web-based application was carried out on the system thoroughly from start to finish of the program. Individual units and components were tested before bringing them together into the whole system which was also tested thoroughly. The different evaluation metric or testing carried out on the prototype is discussed in the subsections below.

3.3.1 Unit Testing

In unit testing each unit of the program were tested to ensure that the program performs its functions as defined in the program specification [22]. A unit is a single testable part of a software system. The aim of unit testing is to validate unit components with its performance [23].

3.3.2 System Testing

System testing is a testing conducted on a complete in-tegrated system to evaluate the system's compliance with its specified requirements [23].

3.3.3 Usability Testing

Usability testing refers to evaluate a software by testing it with representative users. This was done by the users to check that the system meets its supposed requirements [24].

4 Results and Discussion

This chapter provides the proposed system implementation with screenshots for the registration and login process. The system provides easy to use graphics user interface. It also presents all the experiments conducted to evaluate the proposed system and results of the evaluation obtained from the research.

4.1 Registration Interfaces

The registration interfaces which includes upload page, visual cryptography page, data input page and graphical password page are presented in this section.

4.1.1 Upload Page

The sign up interface is the page where the passwords registration takes place. The first page shown for the sign up process is the upload page. The upload interface is shown in Figure 8.

Figure 8. Upload Page

The upload page provides an interface for a user to

select an image of their choice and upload for visual encryption. The browser button in Figure 8 is used to browse the user PC for images. Figure 9 shows the upload page interface after an image has been uploaded by the user.
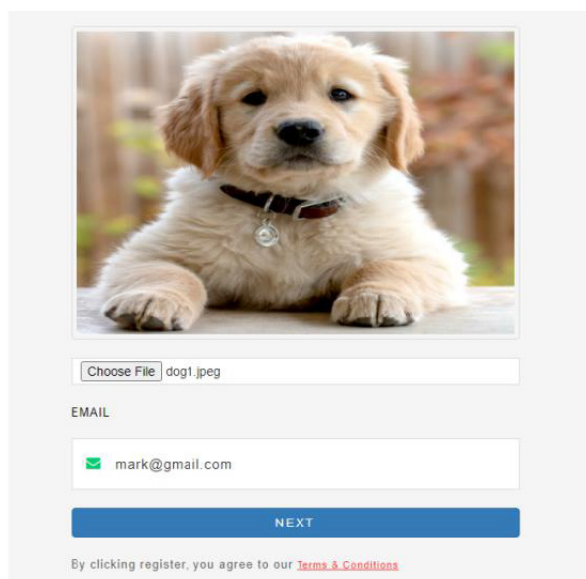

Figure 9. Upload page after user selects and uploads their desired image

4.1.2 Visual Cryptography Page

After uploading the image as shown in Figure 9 the user clicks the next button which leads to the visual cryptography page. The visual cryptography page is shown in Figure 10.
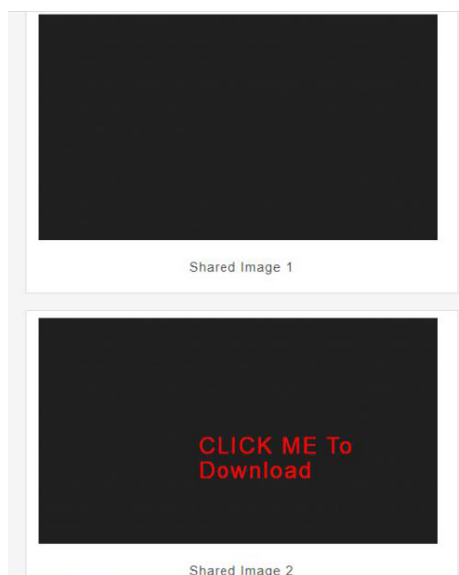

Figure 10. Generated encrypted shared images after performing visual cryptography

The visual cryptography page performance visual

encryption on the image and then generates two shared images. The user is prompted to download the second shared image as shown in red on the second shared image in Figure 10. After downloading the second shared image the user clicks the next button which takes the user to the data input page. The required input data are: username, password, full name, email and phone number. The email address is automatically field based on the email address provided at the upload page. After the user fills the form as all fields are required the user clicks the register button and the user is taken to the graphical password page.

4.1.3 Graphical password registration page

In the graphical password registration page, the user is allowed to registers their graphical password by clicking on their desired images and image grids. The graphical password registration page is illustrated in Figure 11, 12 and 13.
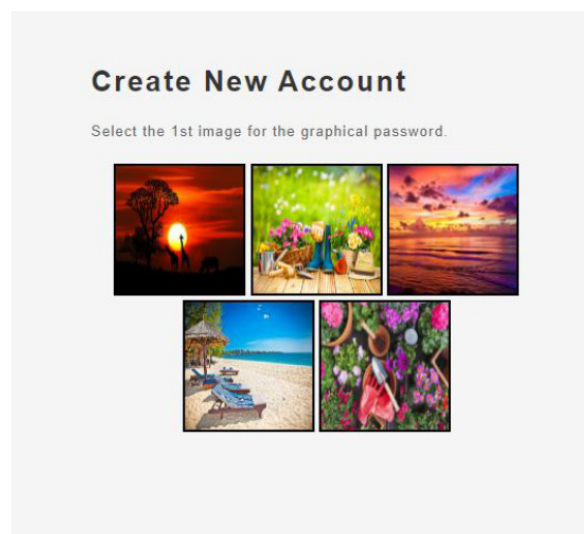

Figure 11. Graphical Password Registration Page

Figure 11 shows the graphical password registration interface with five images displayed. The user is required to click and select one out of this five images. On selecting any of the images, another interface is loaded with four sub-images showing different parts of the selected image. An example of this four sub-images are shown in Figure 12 and Figure 13.

Figure 12 shows four sub-images of the first selected image. The user is required to select one of these four sub-images. After clicking on one of the sub-images, the user is asked to select another image from the five initial images. The second selected image is then divided into four sub-images and the user is prompted to select from this sub-images. The second selected image interface is shown in Figure 13.
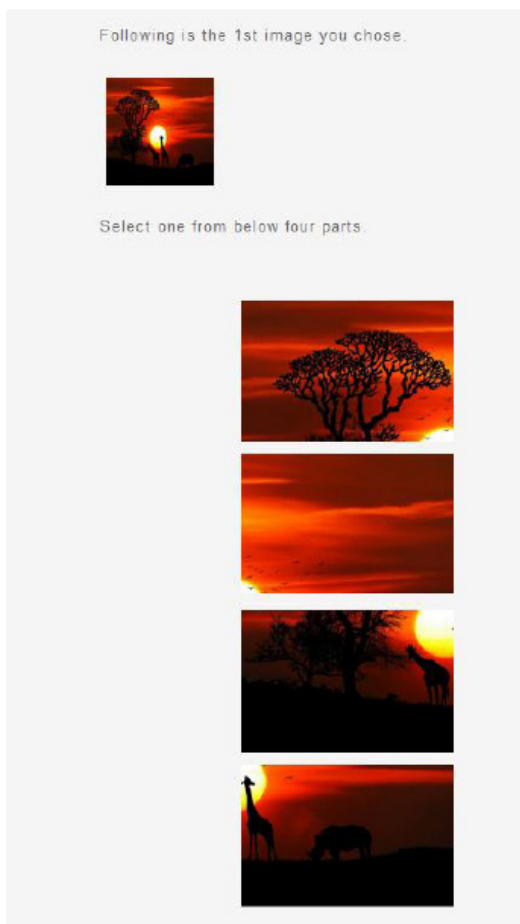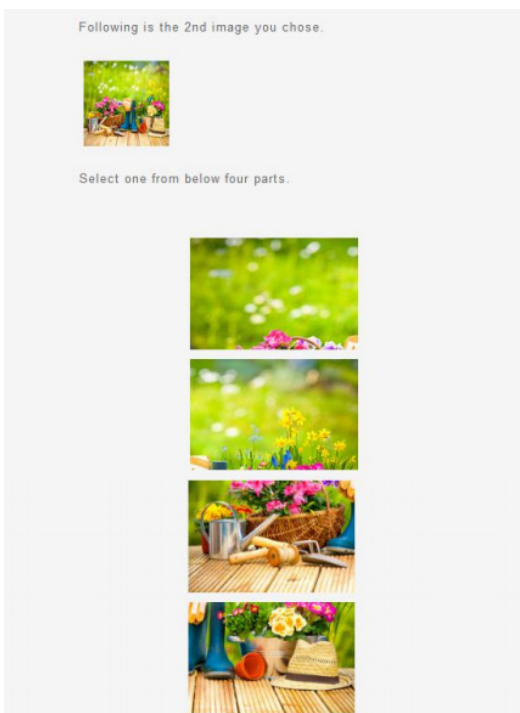
Figure 12. Selected images 4 grids

Figure 13. Second image select by user

4.2 Login Interface

After a user registers their password the user is prompted to login to have access to the web-application. The login interfaces are shown in figures in this section.

4.2.1 Email Validation Page

This is the first page in the login process. In the email validation page the user is required to fill in their registered email. The email validation interface is shown in Figure 14.
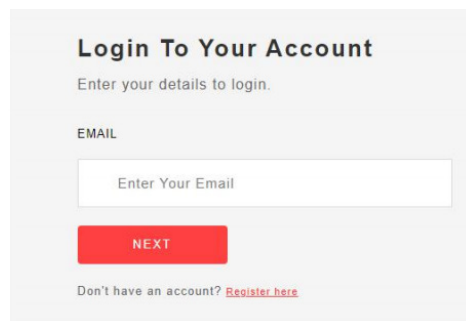

Figure 14. Email Validation Page

If the supplied email address is correct then the user is given access to the decryption page, however if the email is wrong an error message is displayed.

4.2.2 Login Upload Page

After a user's email address is verified the user gets access to the login upload page. The login upload page is a page where a user uploads their downloaded shared image for verification. A sample of the login upload page is shown in Figure 15.
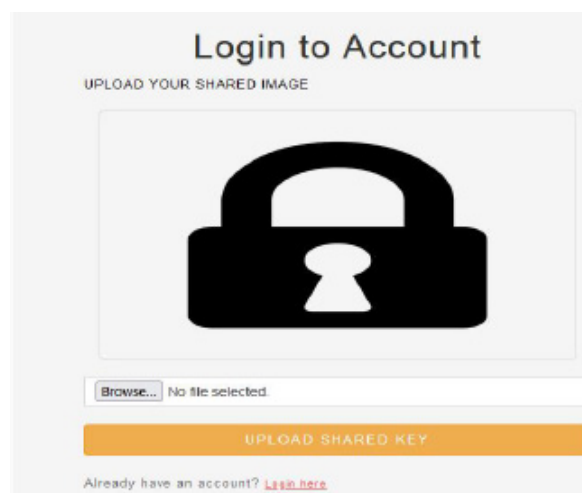

Figure 15. Login Upload Page

The browser button in Figure 15 allows the user to browse their PC and select the downloaded shared images.

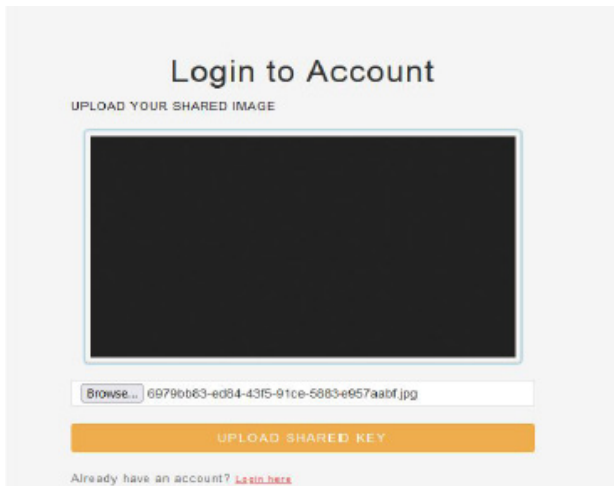Figure 16 shows the interface after the user has selected a shared image.

Figure 16. Login Upload Page after user uploads shared key

After loading the shared image, the user then clicks on the upload share key button which takes the user to the shared image authentication page. If a wrong shared image is uploaded then an error message is outputted and a back button to the login upload page is displayed. If the uploaded shared image is correct then a successful message is shown to the user and a continue button is shown which gives user access to the next phase of authentication.

4.2.3 Username and Password Authentication Page

On successful authentication of the uploaded shared key. The user is asked to enter their username and password on the username and password authentication page. This authentication page is shown in Figure 17.
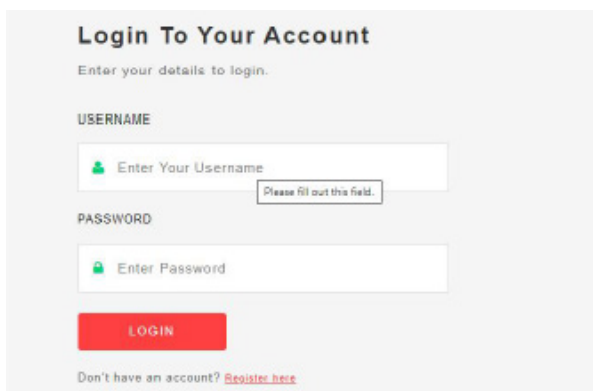

Figure 17. Username and Password Authentication Page

After the user fills in their username and password on click of the login button the inputs are authenticated. If authentication is unsuccessful and error message is displayed and the user is directed to login again. However if the authentication is successful, then the user is redirected to the graphical password page.

4.2.4 Login Graphical Password Page

On the graphical password authentication page the user is required to click on the registered images in same sequence the images were registered during registration. If the wrong graphical password is submitted then user is denied access. If the graphical password is correct then the user is granted access to your profile or the webpage they want to access. The login graphical password page is shown in Figure 18.
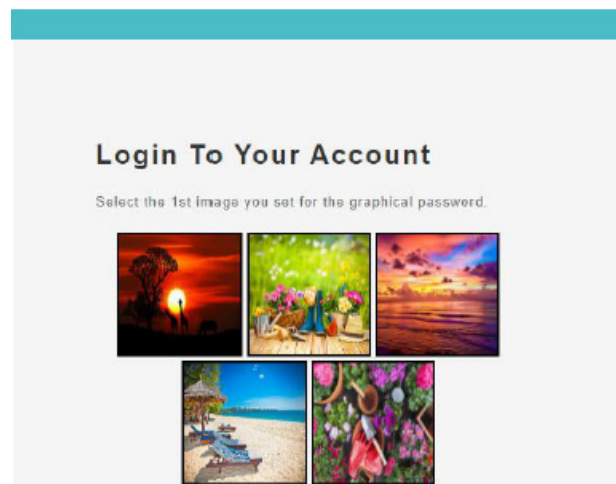

Figure 18. Login Graphical Password Page

4.3 Testing

In this study three types of software testing were conducted. These testing are unit testing, system testing and usability testing. The system was put to the test by a variety of people in terms of functionality and usability. The developer conducted unit and system testing to ensure that each feature and portion of the program and the program as a whole is completely functional. The system was tested by twenty users. Tables 1 and 2 display the results of the system's unit and system testing and usability testing, respectively, to demonstrate that the system meets its specifications.

4.3.1 Unit and System testing

Unit testing deals with testing each software unit to ensure that it performed the functions specified in the program specification. System testing is used to test the functionality of the whole system. The unit and system testing results is presented in Table 1.

Table 1. Unit and System Testing

SECTION	INPUT	EXPECTED RESULT	ACTUAL RESULT	COMMENT
REGISTRATION	Select Image	Allows user to browse images from PC.	Correct	Passed
	Upload Image	Allows user to upload browsed image	Correct	Passed
	Encrypt Image	Allows user to encrypt image using visual cryptography	Correct	Passed
	Download Image	Allows user to download shared image	Correct	Passed
	Fill Sign up form	Allows user to input their details	Correct	Passed
	Submit form	Allows user to submit their details	Correct	Passed
	Click on image to register as password	Allows user click on image to register as password	Correct	Passed
	Save password	System sends and details and passwords to database	Correct	Passed
LOGIN	Enter email address	Allows user to input their email address	Correct	Passed
	Select Shared image	Allows user to browse for shared image from PC.	Correct	Passed
	Upload shared image	Allows user to upload browsed shared image	Correct	Passed
	Authenticate shared image	System authenticates upload shared image	Correct	Passed
	Username and password input	Allow user to input username and password	Correct	Passed
	Authenticate username and password	System verifies the username and password	Correct	Passed
	Select images in sequence	Allow users select images in sequence	Correct	Passed
	Authenticate select images	System authenticates the graphical password	Correct	Passed
USER PROFILE	Change Graphical Password	Enables user to change graphical password	Correct	Passed
	Change text Password	Enables user to change text password	Correct	Passed
	Upload and change profile picture	Allows user to upload and change profile photo	Correct	Passed
SYSTEM TESTING	Registration to user profile process	The completeness of the system from the point of registration to the point of user profile change.	Correct	Passed

4.3.2 Usability Testing

Usability is defined as the degree to which a product allows certain users to achieve their specific goals efficiently, effectively, and satisfactorily in the given context. Usability is an important factor to consider when creating a decent graphical password technique that fulfills the needs and requirements of its users. User given Images, Category of Images, Easy to Use, Easy to Create, Easy to Execute, Nice and Simple Interface, Login Time, and Memorability are some of the primary usability features used in graphical passwords. These usability aspects are described in more detail below.

- **User-assigned Images:** When users are given a password at random, they have a harder time remembering it than when they are given the option to pick their own password.
- **Category of Images:** Users can choose from a variety of image categories based on their personal preferences.
- **Easy to Use:** This refers to the system's ability to provide a good platform for password creation.
- **Easy to Create:** When the registration process is straightforward, people may quickly create their graphical passwords.

- **Easily Executed:** When the registration and login are presented in simple steps, people can easily perform the algorithm.
- **Nice and Simple Interface:** Focuses on the user's interactions rather than the aesthetics of the interface. The goal of a nice and simple interface is to make user interactions as efficient and straightforward as possible.
- **Time to Login:** How long does it take for a user to complete the login process?
- **Memorability:** How easy is it for a person to remember their password?

The system's usability testing based on the six defined features above is presented in Table 2.

Table 2. Usability testing

Usability features	Rating
User assigned Images	High
Category of Images	High
Easy to Use	Moderate
Easy to Create	High
Easily Executed	Moderate
Nice and Simple Interface	High
Login Time	Fast
Memorability	High

5. Conclusions - Future Works

In this study the visual cryptography and cued click point recall-based graphical password techniques were used to perform user's authentication for access to web application. The user authentication system consists of the registration and login phase. The registration phase captures the user's graphical password in sequence, textual password and encrypts the user selected image using visual cryptography. The login phase gives user access to a web application by verifying the authenticity of the user via the submitted encrypted shared image, username, textual password and the submitted sequence of the graphical password. In conclusion, a method for authentication of users for web application was proposed based on visual cryptography and cued click point recall-based graphical password techniques. In this study, authentication using this combined techniques achieved a stronger and reliably security than the existing textual and graphical password systems which are vulnerable to shoulder surfing attack.

The study made use of the cued click point graphical password technique for authentication. For future work other graphical password methods such as the recognition based authentication can be used in combination with the visual cryptography. A disadvantage of graphical password techniques is that it requires more memory space than textual. The visual cryptography also requires large memory space to store the encrypted shared images. A combination of visual cryptography and graphical password in study makes the proposed system memory/space intensive. Hence it is recommended that other encryption methods or authentication methods which requires less memory space be combined with the graphical password technique.

References

[1] P. G. Panduranga Rao, 'A Study of Various Graphical Passwords Authentication Schemes Using Ai Hans Peter Wickelgren Approach', *IOSR J. Comput. Eng.*, vol. 10, no. 6, pp. 14-20, 2013. DOI: 10.9790/0661-1061420.

[2] A. Karode, S. Mistry, and S. Chavan, 'Graphical Password Authentication System', *Int. J. Eng. Res.*, vol. 2, no. 9, p. 4, 2013.

[3] L. Y. Por, C. S. Ku, A. Islam, and T. F. Ang, 'Graphical password: prevent shoulder-surfing attack using digraph substitution rules', *Front. Comput. Sci.*, vol. 11, no. 6, pp. 1098-1108, Dec. 2017. DOI: 10.1007/s11704-016-5472-z.

[4] A. Islam, 'A review of the recognition-based graphical password', p. 11, Jul. 2021.

[5] J. Rajesh, C. Durgesh, W. Milind, and K. Santosh, 'Graphical Password Authentication system', *IJLTEMAS*, vol. 3, p. 5, 2014.

[6] S. Istyaq and M. S. Umar, 'Hybrid Authentication Scheme for Graphical Password Using QR Code and Integrated Sound Signature', vol. 12, no. 2, p. 5, 2018.

[7] Mrs. A. S. Gokhale and V. S. Waghmare, 'The Shoulder Surfing Resistant Graphical Password Authentication Technique', *Procedia Comput. Sci.*, vol. 79, pp. 490-498, 2016. DOI: 10.1016/j.procs.2016.03.063.

[8] S. Shinde and U. H. Wanaskar, 'Keylogging: A Malicious Attack', *Int. J. Adv. Res. Comput. Commun. Eng.*, vol. 5, no. 6, p. 5, Jun. 2016. DOI: 10.17148/IJARCCE.2016.5661.

[9] M. K. Shah, D. Kataria, and S. B. Raj, 'Real Time Working of Keylogger Malware Analysis', *Int. J. Eng. Res.*, vol. 9, no. 10, p. 5, 2020.

[10] C. Santwana and K. S. Aditya, 'Hypervisor based Mitigation Technique for Keylogger Spyware Attacks', vol. 5, p. 4, 2014.

[11] Y. S. Chuen, M. Al-Rashdan, and Q. Al-Maatouk, 'GRAPHICAL PASSWORD STRATEGY', *J. Crit. Rev.*, vol. 7, no. 03, Jan. 2020. DOI: 10.31838/jcr.07.03.19.

[12] A. Vaddeti, D. Vidiyala, V. Puritipati, R. B. Ponnuru, J. S. Shin, and G. R. Alavalapati, 'Graphical passwords: Behind the attainment of goals', *Secur. Priv.*, vol. 3, no. 6, Nov. 2020. DOI: 10.1002/spy2.125.

[13] A. H. Shnain and S. H. Shaheed, 'The Use of Graphical Password to Improve Authentication Problems in E-Commerce', presented at the Proceeding of the 3rd International Conference on Applied Science and Technology, Sep. 2018.

[14] M. Ahsan and Y. Li, 'Graphical Password Authentication using Images Sequence', *Int. Res. J. Enigeering Technol.*, vol. 04, no. 11, p. 9, Nov. 2017.

[15] Dana Yang, I. Doh, and K. Chae, 'Enhanced password processing scheme based on visual cryptography and OCR', in *2017 International Conference on Information Networking (ICOIN)*, Da Nang, Vietnam, 2017, pp. 254-258. DOI: 10.1109/ICOIN.2017.7899514.

[16] B. Togookhuu, W. Li, Y. Sun, and J. Zhang, 'New Graphical Password Scheme Containing Questions- Background-Pattern and Implementation', in *Computer Graphics and Imaging*, IntechOpen, 2019. Accessed: Jul. 05, 2021. [Online]. Available: eativeCommonhttp://creativecommons.org/licenses/

by/3.0.

[17] N. Tiwari and L. Prasad, 'A Comparative Study: Reverse Engineering Flowcharting Tools', vol. 07, no. 01, p. 8, 2015.

[18] V. Vaishnavi, B. Shanthi, and S. S. Rani, 'SECURE DATA SHARING USING VISUAL CRYPTOGRAPHY', vol. 12, no. 1, p. 5, 2017.

[19] P. V. Chavan, M. Atique, and L. Malik, 'Design and Implementation of Hierarchical Visual Cryptography with Expansionless Shares', *Int. J. Netw. Secur. Its Appl.*, vol. 6, no. 1, pp. 91-102, Jan. 2014. DOI: 10.5121/ijnsa.2014.6108.

[20] D. Vaya, S. Khandelwal, and T. Hadpawat, 'Visual Cryptography: A Review', *Int. J. Comput. Appl.*, vol. 174, no. 5, pp. 40-43, Sep. 2017. DOI: 10.5120/ijca2017915406.

[21] V. Moraskar, S. Jaikalyani, M. Saiyyed, J. Gurnani, and K. Pendke, 'Cued Click Point Technique for Graphical Password Authentication', *Int. J. Comput. Sci. Mob. Comput.*, vol. 3, no. 1, pp. 166-172, Jan. 2014.

[22] D. Almog, D. O. V. B. Sohacheski, M. L. Gillenson, R. Poston, and S. Mark, 'THE UNIT TEST : FACING CICD - ARE THEY ELUSIVE DEFINITIONS ?', *J. Inf. Technol. Manag. Publ. Assoc. Manag.*, vol. 29, no. 2, pp. 40-54, 2018.

[23] N. Anwar and S. Kar, 'Review Paper on Various Software Testing Techniques & Strategies', *Glob. J. Comput. Sci. Technol. C Softw. Data Eng.*, vol. 19, no. 2, 2019.

[24] A. Elsafi, D. N. A. Jawawi, A. Abdelmaboud, and A. Ali, 'A comparative evaluation of state-of-the-art integration testing techniques of component-based software', *J. Theor. Appl. Inf. Technol.*, vol. 71, no. 2, pp. 257-267, 2015.

ARTICLE

Intrusion Detection through DCSYS Propagation Compared to Auto-encoders

Fatima Isiaka[1*]   Zainab Adamu[2]

1. Department of Computer Science, Nasarawa State University, Keffi, Nigeria
2. Department of Computer Science, Ahmadu Bello University, Zaria, Nigeria

ABSTRACT

In network settings, one of the major disadvantages that threaten the network protocols is the insecurity. In most cases, unscrupulous people or bad actors can access information through unsecured connections by planting software or what we call malicious software otherwise anomalies. The presence of anomalies is also one of the disadvantages, internet users are constantly plagued by virus on their system and get activated when a harmless link is clicked on, this a case of true benign detected as false. Deep learning is very adept at dealing with such cases, but sometimes it has its own faults when dealing benign cases. Here we tend to adopt a dynamic control system (DCSYS) that addresses data packets based on benign scenario to truly report on false benign and exclude anomalies. Its performance is compared with artificial neural network auto-encoders to define its predictive power. Results show that though physical systems can adapt securely, it can be used for network data packets to identify true benign cases.

1. Introduction

This paper contains an introductory viewpoint to network security, different threats to a network setting, deep learning and the design of different autonomous systems for network security. The goal is to approach this in a simplified form, by first taking a look at the different forms of threats, understanding deep learning and using deep learning in development of safe and autonomous systems for a safe network. This section contains an overview of network security, threats and deep learning with Auto encoders and an overview of Dynamic Control System (DCSYS).

One of the major disadvantages of a network setting is the insecurity. If the internet can be used for online banking, social networking and other services, one may risk a theft to personal information such as name, credit card information, address e.t.c. Unscrupulous people or bad actors can access these information through unsecured connections by planting software or what we call malicious software and use personal details for their benefit. The presence of anomalies is one of the disadvantages. Internet users are constantly plagued by virus on their system and get deactivated when a harmless link is clicked on (true benign case). Most computers connected to internet are always very prone to targeted virus attacks and they often end up getting crashed Unfortunately, the ability to send and receive mails created a means for cyber criminals

Corresponding Author:
Fatima Isiaka,
Department of Computer Science, Nasarawa State University, Keffi, Nigeria;
Email: fatima.isiaka@outlook.com

to off-load anomalies. Some malware attached to emails could wreak havoc to computers and create backdoor for attackers to infiltrate the network system. The attackers can lure victims into disclosing sensitive information through techniques like phishing scams. The on-going evolvement and introduction of new and advanced threats to network systems have called for the need to build autonomous, safe and interactive systems that can counteract unauthorised access, attacks and access true benign case without false alert. To address this, the paper seeks to discourse the following objectives:

- address cases of false positive in an actual benign scenario.
- reduce the occurrence of advanced threats.
- create a dynamic control intrusion detection system (DCSYS).
- compare its performance with ANN auto-encoders.

These systems will be as a form of interactive tool in a controlled environment that can filter out anomalies, virus intrusion and reproduce interceptions protocols that identifies true benign cases.

1.1 Auto Encoders

In an intrusion detection system (IDS), one of its most positive rule is being able to identify when the configuration has changed or when some network traffic indicates a problem such as when capital one data has been breached (Figure 1). Artificial neural network (ANN) is one of the most faultless IDS as a Deeping learning method and a typical auto-encoder (AE) is a type of ANN used to learn efficient data coding in an unsupervised tender manner [1-4]. Its aim is to learn a representation or encoding for a set of prime data, which is typically for dimensional reduction. Training the network to ignore outlying cases is one its characteristics. Also the reconstruction side is learned, here the auto-encoder generates from the reduced encoding by representing its original input [5-8]. The AE are applied to a lot of problems from facial recognition to acquiring the class semantic meaning and representation of words. It can serve as form of feedback loop for network security data analysis [10,11] for pre-served browsing activities online. One of its equivalent is the variational encoder, a model based on ANN that provides probabilistic manner for describing an observation in a constant latent space. Ultimately, rather than building an encoder which outputs a single value to describe each latent state features, an encoding characteristics can be formulated that describe a probability distribution for each latent class of attributes. Figure 2 shows a typical network architecture for an auto-encoder with μ and σ as the latent class of attributes that produces new set of classes . The variational auto-encoder is a neural network where the middle layer of the network is made of mean and standard deviation that are sampled from the normal distribution derived from input parameters. In AE and VAE all layers use state-of-the-art convolutional neural networks which can be made explicit with inclusion of hyper-parameters as shown in the diagrams below for both AE and VAE.

Despite the deep learning applications to IDS, there are some of its drawbacks such as identifying true benign cases which are sometimes detected as false positive. Here we tend to apply a dynamic control system that can deal with such case and compare its performance to auto-encoders.

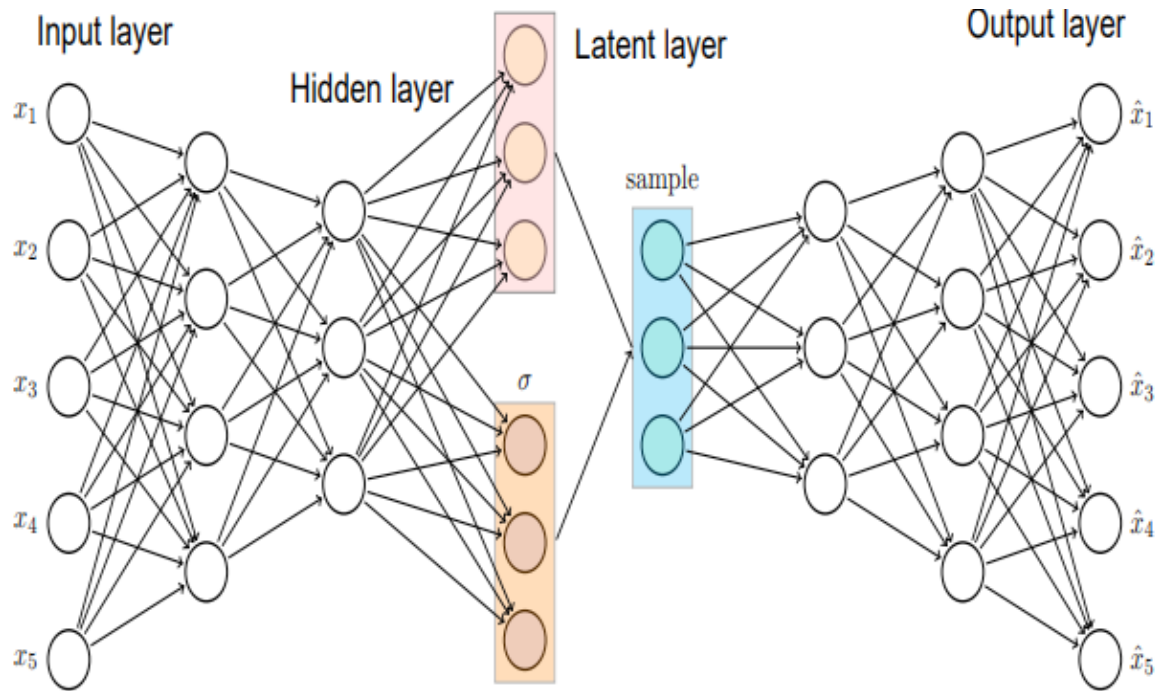**Figure 1.** Capital one data breach (Curtsey: Google image)

Figure 2. A High-level illustration of AE with hidden and latent layers.

1.2 Dynamic Control Systems

Dynamic control systems are based on discrete time-variant computation which are well known for dealing with physical systems that result in perfect detected signals [11-13]. A dynamic control system manages the command, direction, and regulates the behaviour of other systems using its control loops. It can range from a controller used for controlling processes or machines and powered systems.

The models are comprised of a linear feedback systems, a control loop which includes control algorithms and actuators that attempt to regulate variable set-point (SP). An example is a PID controller algorithm [12,9,10] that controls and restores an actual instance of speed process to the desired speed in an optimum level, with minimal delay or false alert, by controlling the predicted power output of an engine controlling process.

1.3 The Proposed DCSYS Model

The setup function allows for the input of data not limited to the CICA dataset but for a generalised scenario. Predictions are made based on the benign and non-benign cases from an identity state space model set, used as input.

Here we intend to use the control model's process formation to help fish-out false benign cases and comparing its predictive ability with auto-encoders. A window-based control panel was designed as a standalone, solely to address true benign case in the Canadian Institute for Network Security (CICA) data.
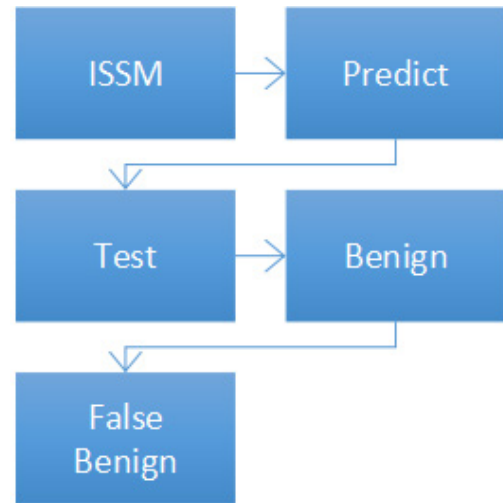

Figure 3. Model Kernel for DCSYS.

2. Method and Dataset

The CICA dataset (Figure 3) contains benign cases that leaves room to address false positive, the "Benign" cases were treated as a single entity to differentiate between "false benign" and "true benign" case. The DCSYS model is encapsulated has an identified state space model given as:

$$\frac{dx}{dy}(t) = Ax(t) + Bu(t) + K\,e(t)$$
$$y(t) = Cx(t) + Du(t) + e(t) \tag{1}$$

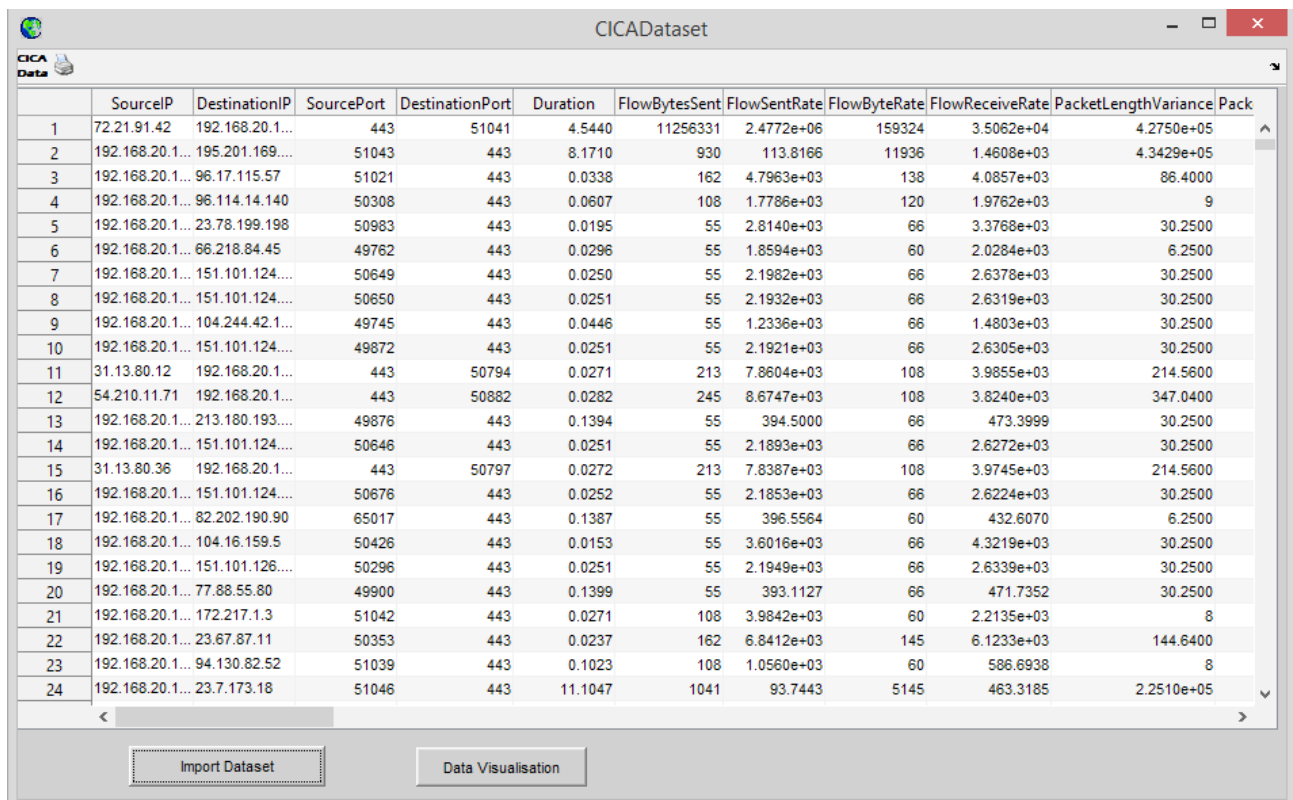where are the state space converted matrices, *u(t)* is the

input attributes or data packet features, *y(t)* is the output, *e(t)* denotes the disturbance and *x(t)* the vector matrix of signal propagation. All state space matrices are considered free parameters. The matrix is set to zero value, which means no feed-through by default except for the static systems. The default behaviour of the system is modified by feed-through and disturbance pairs. The DCSYS is modified using an interactive form that inputs datasets for visualisation and analysis.

The CICA dataset is a time series data transformed into an identified data series, containing a time-domain output signal *y* and an empty input signal respectively. The sampling interval is specified using an arbitrary constant parameter for the dataset. The output data by default have the same domain as the input data.

The DCSYS takes in data packet and generates an alert (Figure 5) whenever a "false benign" is detected, this report is generated from the denial of serves features created from the data packet. The corresponding source port and destination port is then identified and relays options for either blocking or deleting the data packet associated to these addresses. All cases are treated as benign on till a false case is encountered. The identified matrix created from the data packet is then run through the DCSYS (Fig-

ure 6) which generates report on the discrete time identified state space model (MDL) and the ROC or performance of the detection session, this is to authenticate the genuinety of the report and the area under the curve (AUC) transmits the models performance. Bode reports show the frequency response, magnitude, phase of frequency response and the predictive power of each feature attributed to the CICA data, this leaves room for which attribute contributes to the predictive ability of the system or which attribute is impassive. From the Figure 5, the data attribute "*Packet Length Median*" to the "*Source Port*" seem to contribute most significantly to the models predictive power that addresses false benign cases. The system can also generate report on whether exclusion of anomalies and attributes is pre-eminent for the model.

To generalise the predictive performance of the model, a plain comparative analysis is demonstrated with ANN auto-encoders on different epochs (*2, 3, 4*) and *order 1-3* for the DCSYS model on four different scenarios (for anomalies removed, anomalies included, four authentic attributes with anomalies included, and dataset with all attributes). The proceeding the section discusses the results obtained from the analysis as compared to an auto-encoder.

		SourceIP	DestinationIP	SourcePort	DestinationPort	Duration	FlowBytesSent	FlowSentRate	FlowByteRate	FlowReceiveRate	PacketLengthVariance	Pack
1		72.21.91.42	192.168.20.1...	443	51041	4.5440	11256331	2.4772e+06	159324	3.5062e+04	4.2750e+05	
2		192.168.20.1...	195.201.169....	51043	443	8.1710	930	113.8166	11936	1.4608e+03	4.3429e+05	
3		192.168.20.1...	96.17.115.57	51021	443	0.0338	162	4.7963e+03	138	4.0857e+03	86.4000	
4		192.168.20.1...	96.114.14.140	50308	443	0.0607	108	1.7786e+03	120	1.9762e+03	9	
5		192.168.20.1...	23.78.199.198	50983	443	0.0195	55	2.8140e+03	66	3.3768e+03	30.2500	
6		192.168.20.1...	66.218.84.45	49762	443	0.0296	55	1.8594e+03	60	2.0284e+03	6.2500	
7		192.168.20.1...	151.101.124....	50649	443	0.0250	55	2.1982e+03	66	2.6378e+03	30.2500	
8		192.168.20.1...	151.101.124....	50650	443	0.0251	55	2.1932e+03	66	2.6319e+03	30.2500	
9		192.168.20.1...	104.244.42.1...	49745	443	0.0446	55	1.2336e+03	66	1.4803e+03	30.2500	
10		192.168.20.1...	151.101.124....	49872	443	0.0251	55	2.1921e+03	66	2.6305e+03	30.2500	
11		31.13.80.12	192.168.20.1...	443	50794	0.0271	213	7.8604e+03	108	3.9855e+03	214.5600	
12		54.210.11.71	192.168.20.1...	443	50882	0.0282	245	8.6747e+03	108	3.8240e+03	347.0400	
13		192.168.20.1...	213.180.193....	49876	443	0.1394	55	394.5000	66	473.3999	30.2500	
14		192.168.20.1...	151.101.124....	50646	443	0.0251	55	2.1893e+03	66	2.6272e+03	30.2500	
15		31.13.80.36	192.168.20.1...	443	50797	0.0272	213	7.8387e+03	108	3.9745e+03	214.5600	
16		192.168.20.1...	151.101.124....	50676	443	0.0252	55	2.1853e+03	66	2.6224e+03	30.2500	
17		192.168.20.1...	82.202.190.90	65017	443	0.1387	55	396.5564	60	432.6070	6.2500	
18		192.168.20.1...	104.16.159.5	50426	443	0.0153	55	3.6016e+03	66	4.3219e+03	30.2500	
19		192.168.20.1...	151.101.126....	50296	443	0.0251	55	2.1949e+03	66	2.6339e+03	30.2500	
20		192.168.20.1...	77.88.55.80	49900	443	0.1399	55	393.1127	66	471.7352	30.2500	
21		192.168.20.1...	172.217.1.3	51042	443	0.0271	108	3.9842e+03	60	2.2135e+03	8	
22		192.168.20.1...	23.67.87.11	50353	443	0.0237	162	6.8412e+03	145	6.1233e+03	144.6400	
23		192.168.20.1...	94.130.82.52	51039	443	0.1023	108	1.0560e+03	60	586.6938	8	
24		192.168.20.1...	23.7.173.18	51046	443	11.1047	1041	93.7443	5145	463.3185	2.2510e+05	

Import Dataset   Data Visualisation
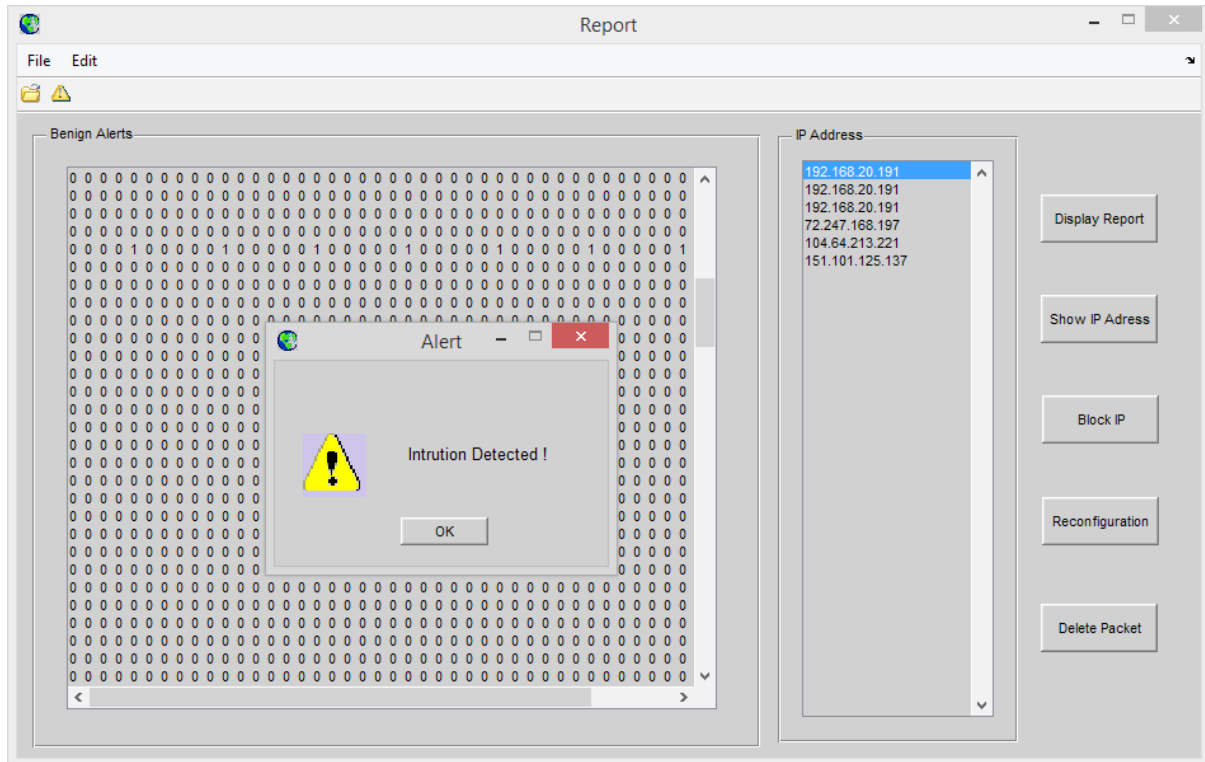
Figure 4. The Canadian Network Security Database

Figure 5. Data message report screen for data packets.
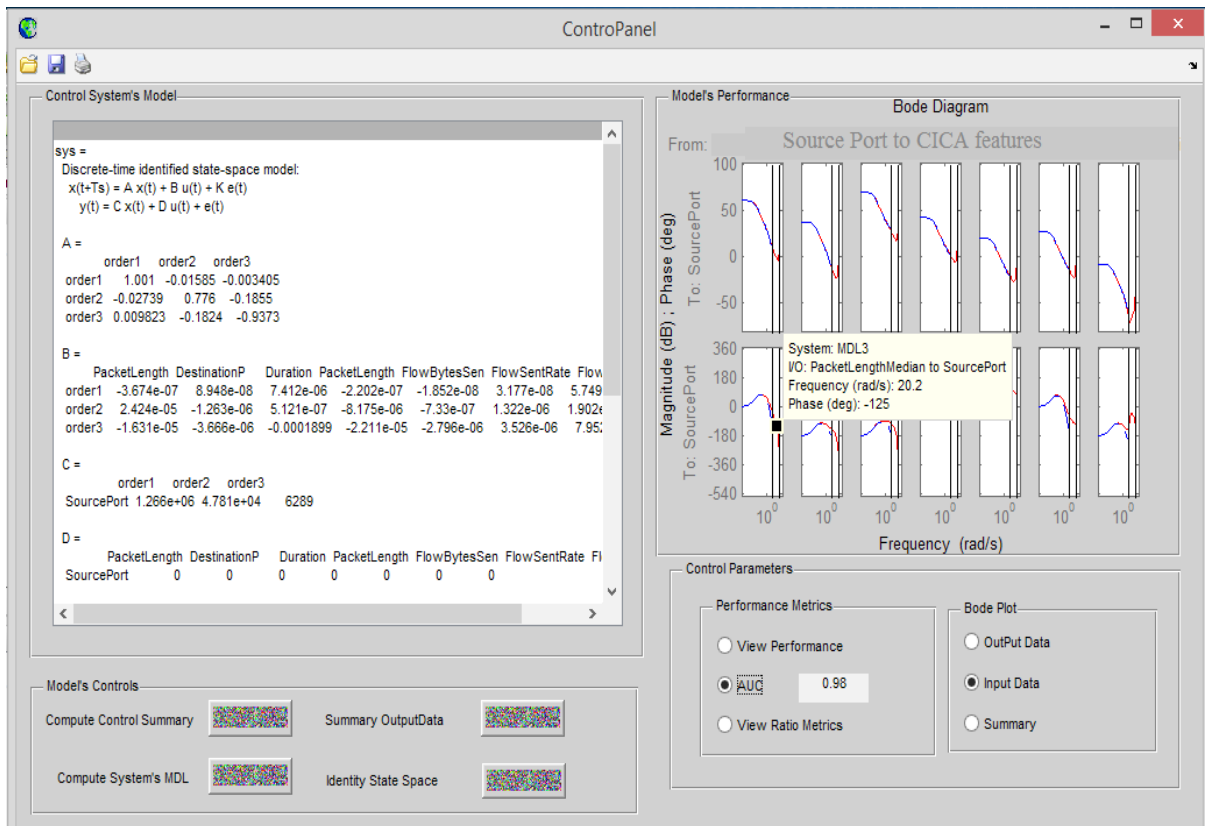

Figure 6. Control panel for report generator on the discrete time identified state space model (MDL).

3. Results

The Receiver Operating Characteristics (ROC) Curve comparison for DCSYS and Auto-encoders at different order and epochs for anomalies removed shows that DCSYS outperforms the auto-encoder with *0.90* accuracy at order one and *0.80* at order three (Figure 7). The auto encoder has an accuracy of *0.70*. This shows a close performance.

As compared to anomalies included, the ROC curve comparison for DCSYS and Auto-encoders at different order and epochs shows a performance of *0.90* and *0.80* for the DCSYS that outperforms the auto-encoders (Figure 8). The ROC Curve Comparison for DCSYS and Auto-encoders at different order and epochs for four authentic attributes shows a performance of *0.80* for the auto-encoder at three epoch and very low performance for the
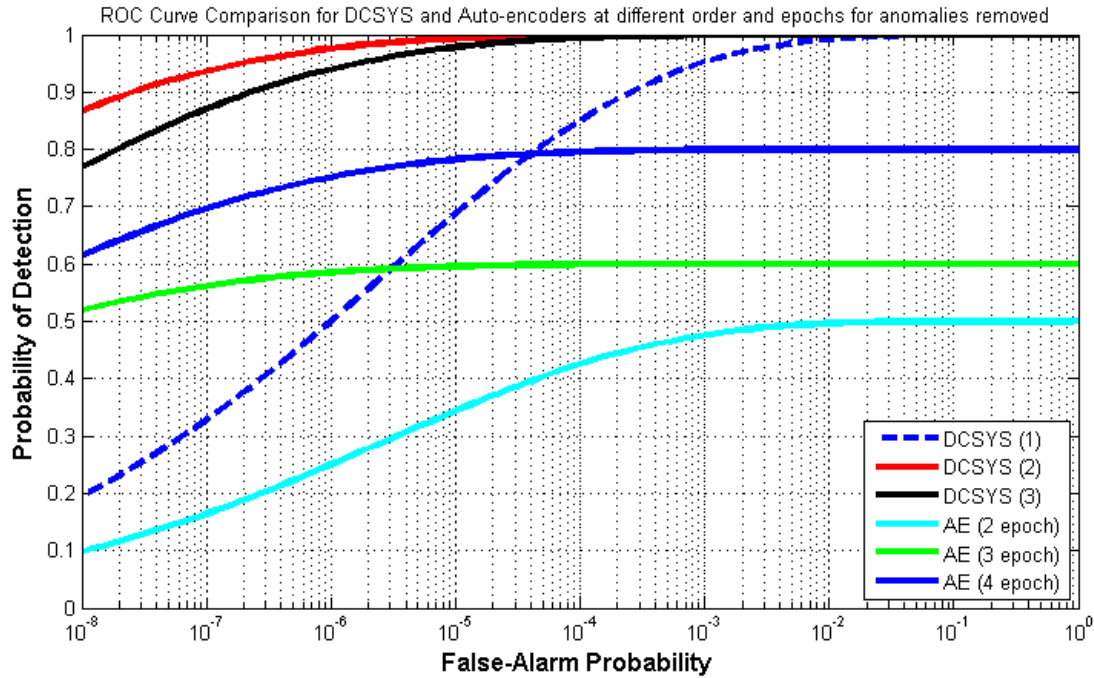

Figure 7. ROC Curve Comparison for DCSYS and Auto-encoders at different order and epochs for anomalies removed in Benign scenario 1.
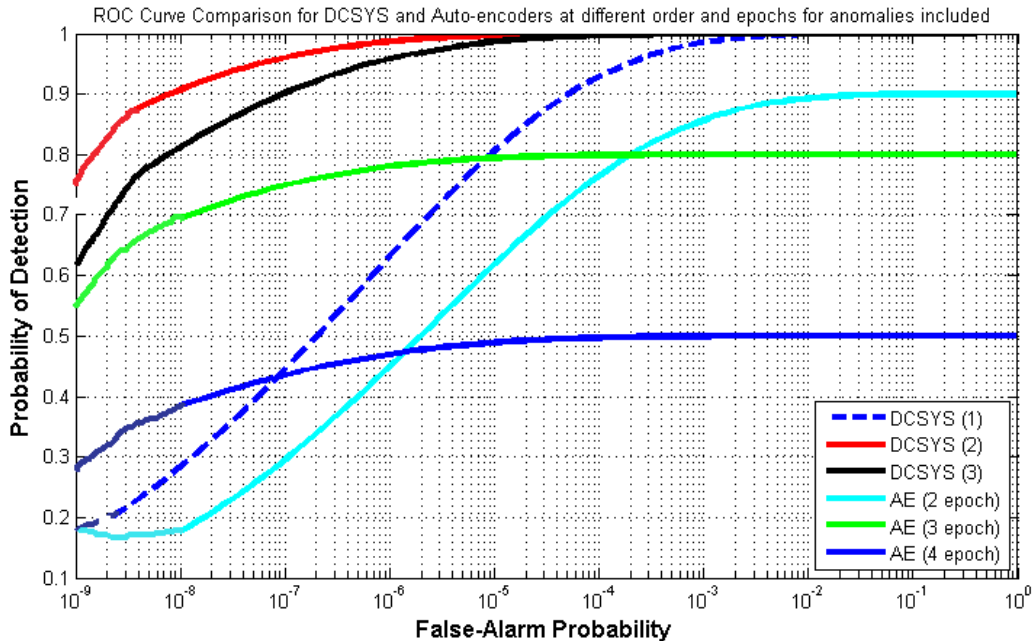

Figure 8. ROC Curve Comparison for DCSYS and Auto-encoders at different order and epochs for anomalies included in Benign scenario 2.

DCSYS (Figure 9), the auto-encoder's detection ability of false alarm is intensified for the case of authenticity of the CICA dataset's features as when compared to the control system's models predictive power. The ROC curve com-

parison for DCSYS and Auto-encoders at different order and epochs for dataset with all attributes included (Figure 10) shows that the DCSYS outperformances the auto-encoders. The overall predictive performance is in favour of
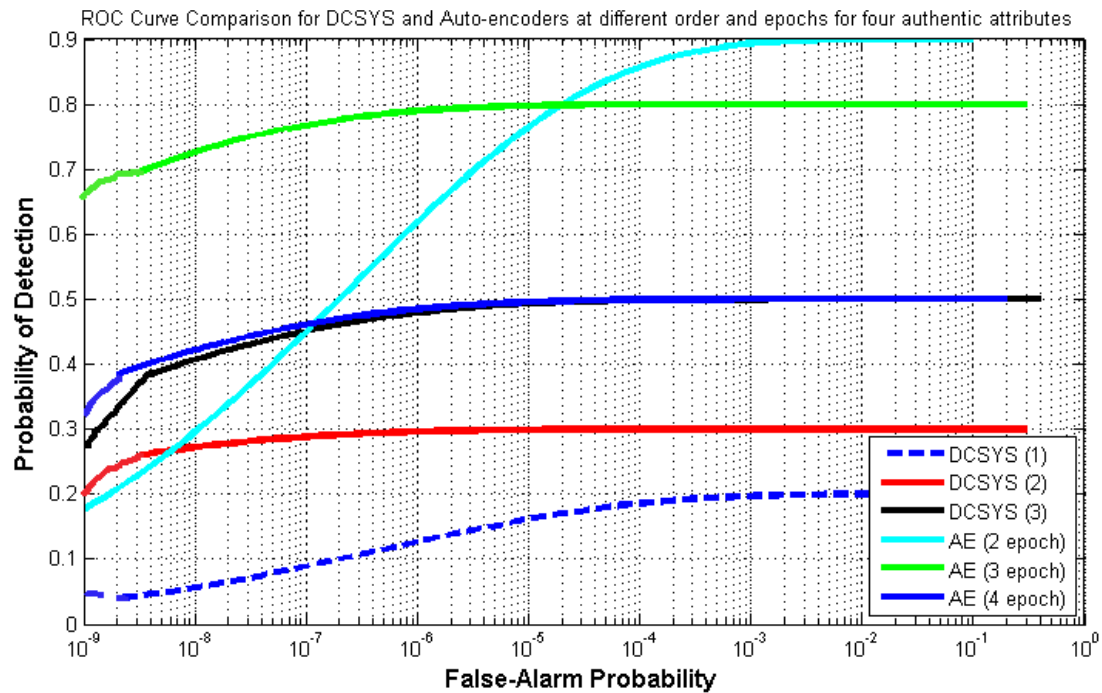

Figure 9. ROC Curve Comparison for DCSYS and Auto-encoders at different order and epochs for four authentic attributes in Benign scenario 3.
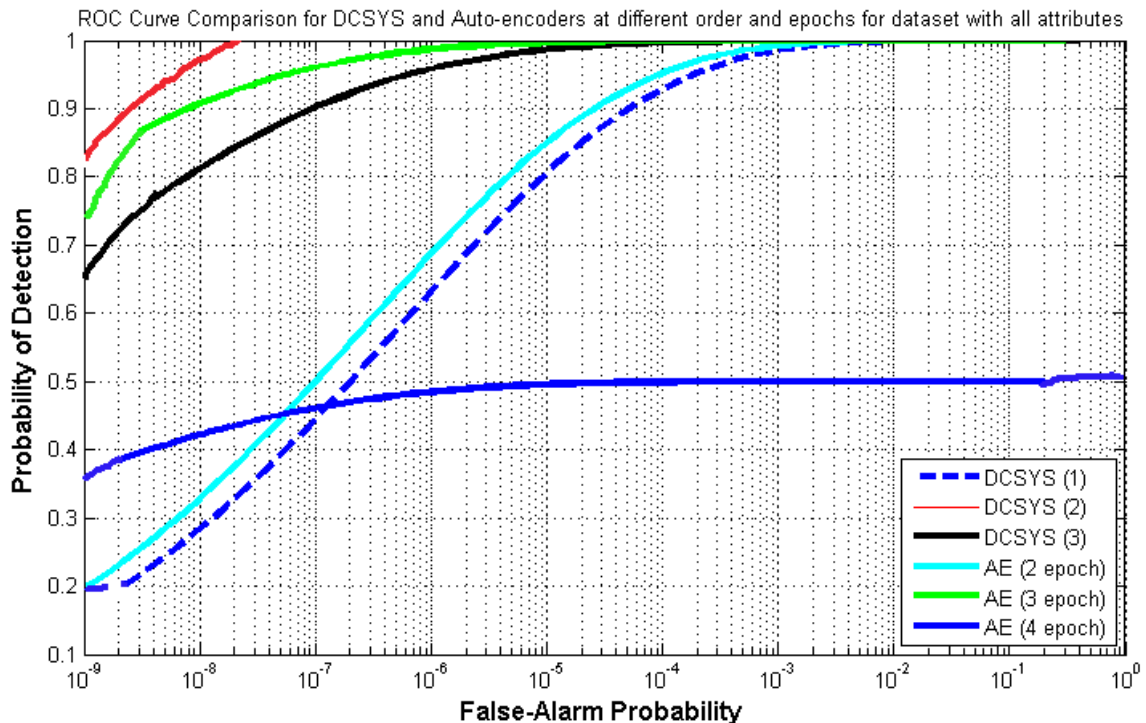

Figure 10. ROC Curve Comparison for DCSYS and Auto-encoders at different order and epochs for datasets with all the attributes in Benign scenario 4.

the DCSYS in the case of redundant features.

4. Conclusions

This paper seeks to investigate IDS with DCSYS propagation in a network setting that involves a CICA data packet. As discussed in the paper, one of the major disadvantages that threaten the network protocols is the insecurity. In most cases, bad actors can access information through unsecured connections by planting software or what we call malicious software otherwise identified as anomalies which can be presented as false benign in a benign oriented scenario. The presence of these anomalies is one of the disadvantages. Internet users are constantly plagued by this false benign cases on their system and get activated when a harmless link is clicked on. Deep learning is very adept at dealing with such cases, but sometimes it has its own fault when dealing with benign cases. The paper tends to adopt a dynamic control system (DCSYS) that addresses data packets based on benign scenario to truly report on false benign and exclude anomalies. To define its predictive ability, its performance is compared with an auto-encoder on different epochs. Results show that performance of 0.9 above is quite adaptive enough to validate its predictive ability. Though physical systems can adjust securely, it can be used for network data packets to identify true benign cases. Future work is to further compare its performance with both recurrent and convolutional neural network and improve its performance metrics as a standalone tool that could be embed in an IDS.

References

[1] Phan, N., Wang, Y., Wu, X., & Dou, D. (2016, February). Differential privacy preservation for deep auto-encoders: an application of human behavior prediction. In *Thirtieth AAAI Conference on Artificial Intelligence*.

[2] Kipf, T. N., & Welling, M. (2016). Variational graph auto-encoders. *arXiv preprint arXiv:1611.07308*.

[3] Soui, M., Smiti, S., Mkaouer, M. W., & Ejbali, R. (2020). Bankruptcy prediction using stacked auto-encoders. *Applied Artificial Intelligence*, *34*(1), 80-100.

[4] Ding, Y., Tian, L. P., Lei, X., Liao, B., & Wu, F. X. (2021). Variational graph auto-encoders for miR-NA-disease association prediction. *Methods*, *192*, 25-34.

[5] Wang, W., & Gómez-Bombarelli, R. (2019). Coarse-graining auto-encoders for molecular dynamics. *npj Computational Materials*, *5*(1), 1-9.

[6] Wu, X., & Cheng, Q. (2021). Deepened Graph Auto-Encoders Help Stabilize and Enhance Link Prediction. *arXiv preprint arXiv:2103.11414*.

[7] Wu, X., & Cheng, Q. (2021). Deepened Graph Auto-Encoders Help Stabilize and Enhance Link Prediction. *arXiv preprint arXiv:2103.11414*.

[8] Gomede, E., de Barros, R. M., & de Souza Mendes, L. (2021). Deep auto encoders to adaptive e-learning recommender system. *Computers and Education: Artificial Intelligence*, *2*, 100009.

[9] Silva, A. B. O. V., & Spinosa, E. J. (2021). Graph Convolutional Auto-Encoders for predicting novel lncRNA-Disease associations. *IEEE/ACM Transactions on Computational Biology and Bioinformatics*.

[10] Arifoglu, D., Wang, Y., & Bouchachia, A. (2021). Detection of Dementia-Related Abnormal Behaviour Using Recursive Auto-Encoders. *Sensors*, *21*(1), 260.

[11] Zino, L., & Cao, M. (2021). Analysis, prediction, and control of epidemics: A survey from scalar to dynamic network models. *arXiv preprint arXiv:2103.00181*.

[12] Zhou, P., Chen, W., Yi, C., Jiang, Z., Yang, T., & Chai, T. (2021). Fast just-in-time-learning recursive multi-output LSSVR for quality prediction and control of multivariable dynamic systems. *Engineering Applications of Artificial Intelligence*, *100*, 104168.

[13] Sun, C., Chen, J., Cao, S., Gao, X., Xia, G., Qi, C., & Wu, X. (2021). A Dynamic Control Strategy of District Heating Substations Based on Online Prediction and Indoor Temperature Feedback. *Energy*, 121228.